Modulation of voltage-dependent K^+ conductances in photoreceptors trades off investment in contrast gain for bandwidth

Francisco J. H. Heras[1,+,*], Mikko Vähäsöyrinki[2], and Jeremy E. Niven[3,4,*]

[1]Department of Zoology, University of Cambridge, Cambridge CB2 3EJ, UK
[2]Sensapex Ltd, Oulu, Finland
[3]School of Life Sciences, University of Sussex, Falmer, Brighton BN1 9QG, UK.
[4]Centre for Computational Neuroscience and Robotics, University of Sussex, Falmer, Brighton BN1 9QG, UK.
[+]Current address: Champalimaud Research, Champalimaud Center for the Unknown, 1400-038 Lisbon, Portugal
[*]Correspondence: fjhheras@gmail.com / J.E.Niven@sussex.ac.uk

June 11, 2018

Abstract

Modulation is essential for adjusting neurons to prevailing conditions and differing demands. Yet understanding how modulators adjust neuronal properties to alter information processing remains unclear, as is the impact of neuromodulation on energy consumption. Here we combine two computational models, one Hodgkin-Huxley type and the other analytic, to investigate the effects of neuromodulation upon *Drosophila melanogaster* photoreceptors. Voltage-dependent K^+ conductances: (i) activate upon depolarisation to reduce membrane resistance and adjust bandwidth to functional requirements; (ii) produce negative feedback to increase bandwidth in an energy efficient way; (iii) produce shunt-peaking thereby increasing the membrane gain bandwidth product; and (iv) inactivate to amplify low frequencies. Through their effects on the voltage-dependent K^+ conductances, three modulators, serotonin, calmodulin and PIP2, trade-off voltage-contrast gain against membrane bandwidth. Serotonin shifts the photoreceptor performance towards higher voltage-contrast gains and lower membrane bandwidths, whereas PIP2 and calmodulin shifts performance towards lower voltage-contrast gains and higher membrane bandwidths. These neuromodulators have little effect upon the overall energy consumed by photoreceptors, instead they redistribute the energy invested in gain versus bandwidth. This demonstrates how modulators can shift neuronal information processing within the limitations of biophysics and energy consumption.

1 Introduction

The activity of neurons and neural circuits is modulated to adjust their properties to changes in state, affecting behaviour. Modulation can occur at large spatial scales, encompassing large numbers of neurons, or may be more localised, being restricted to small circuits or single neurons (Harris-Warrick and Marder, 1991; Katz, 1999; Nusbaum and Beenhakker, 2002; Marder, 2011; Marder et al., 2014). It can be brief or prolonged, and may be intrinsic or extrinsic to the circuits being modulated. A variety of substances from small gases (e.g. NO) to biogenic amines (e.g. serotonin, dopamine), peptides (e.g. FMRFamide) and other small molecules (e.g. ATP, PIP2) can act as modulators (Katz, 1999), altering their biophysical properties and, by doing so, affecting electrical signalling in neurons.

Many studies have focussed on the specific effects of modulators on voltage-dependent conductances, quantifying their effects on signalling and, in some cases, on behaviour (Katz, 1999). For example, by acting on voltage-dependent conductances modulators can switch interneurons and motor neurons from following synaptic inputs directly to generating intrinsic bursting rhythms (Weimann and Marder, 1994). Studies of sensory neurons have also shown that modulators can alter their gain and frequency response (bandwidth), as well as increasing their coding precision (Billimoria et al., 2006). But despite extensive characterisation of the coding benefits and behavioural consequences of modulating voltage-dependent conductances, the energy costs of doing so have been largely ignored.

Voltage-dependent conductances make a major contribution to neuronal energy consumption because their properties determine the flux of ions crossing the bilipid membrane to generate electrical signals, whether pre- or postsynaptic (Laughlin, 2001; Niven and Laughlin, 2008; Niven, 2016). Ion flux is related to energy consumption primarily through the work done by the Na^+/ K^+ pump, which is powered by the hydrolysis of ATP molecules (Kety, 1957; Skou, 1957). Thus, by altering ion flux, the modulation of voltage-dependent conductances may affect neuronal energy consumption and the energy efficiency of electrical signalling.

Here we assess this possibility in the R1-6 photoreceptors of the fruit fly, *Drosophila melanogaster*, using an analytic computational model of the photoreceptor to understand and interpret the biophysics accompanied by a

Hodgkin-Huxley-type model to assess energy costs. The models incorporate the voltage-dependent K^+ conductances expressed by these photoreceptors: a rapidly inactivating conductance encoded by the Shaker gene; a more slowly inactivating conductance encoded by the Shab gene; and, a non-inactivating conductance of unknown provenance (the 'novel' conductance) (Hardie, 1991; Vähäsöyrinki et al., 2006). Fruit fly photoreceptors, like those of other insects, encode information contained in light as a graded depolarisation. Consequently, voltage-dependent K^+ conductances can change the filter properties of the membrane, altering the gain and bandwidth of electrical signals and have recently been shown to improve energy efficiency (Weckström and Laughlin, 1995; Niven et al., 2003a; Niven et al., 2003b; Vähäsöyrinki et al., 2006; Heras et al., 2016; Heras et al., 2017). The Shaker and Shab voltage-dependent K^+ conductances of fruit fly photoreceptors are modulated by serotonin and PIP2 (Hevers and Hardie, 1995; Kauranen and Weckström, 2004; Krause et al., 2008). This provides an opportunity to characterise the changes in electrical signalling wrought by modulators in fruit fly photoreceptors, and determine whether such changes produce substantial effects upon energy consumption and efficiency.

2 Methods

2.1 Hodgkin-Huxley characteristics of the K^+ voltage-dependent conductances

We used a Hodgkin-Huxley (HH) formulation (Hodgkin and Huxley, 1952) to model the dynamics of the three voltage-dependent K^+ conductances present in the fruit fly, *Drosophila melanogaster*, R1-6 photoreceptors. Activation and inactivation rates were obtained from previous studies (Niven et al., 2003b; Kauranen and Weckström, 2004; Vähäsöyrinki et al., 2006). In the following formulae describing conductance properties, steady-state activation and inactivation gating variables have no units, the voltage, V, is given in mV and the time constants are given in ms.

2.1.1 Shaker

The fast-activating and fast-inactivating conductance encoded by *Shaker* has conductance $g_{\mathrm{K,Shaker}} = \overline{g_{\mathrm{K,Shaker}}} h m^3$. The activation gating variable, m, has the following steady-state properties (Kauranen and Weckström, 2004):

$$m_\infty(V) = \left[\frac{1}{1+\exp\left(\frac{-23.7-V}{12.8}\right)}\right]^{1/3} \tag{1}$$

$$\tau_m(V) = \frac{1}{0.00817\,\exp\left(\frac{-V+1.62}{24.7}\right) + 0.0581\frac{-V-59.6}{\exp\left(\frac{-V-59.6}{4.50}\right)-1}} \tag{2}$$

The inactivation gating variable h is the sum of two components, $h = \xi + (1-\xi)h_1$. The first one is constant, representing the fraction of Shaker that fails to inactivate, which is $\xi = 0.13$. The second one is a HH variable with the following steady-state properties:

$$h_{1,\infty}(V) = \frac{0.8}{1+\exp\left(\frac{55.3+V}{3.9}\right)} + \frac{0.2}{1+\exp\left(\frac{74.8+V}{10.7}\right)} \tag{3}$$

$$\tau_{h,1}(V) = \frac{1}{0.230\,\exp\left(\frac{-V-193.0}{31.3}\right) + 0.0437\frac{-V+13.5}{\exp\left(\frac{-V+13.5}{11.1}\right)-1}} \tag{4}$$

Serotonin produces a change in Shaker conductance properties (Figure 1). The activation time constant is shifted by 31.4 mV towards more positive voltages, while inactivation is shifted by 25 mV, with a small correction in shape (Hevers and Hardie, 1995):

$$m_\infty(V) = \left[\frac{1}{1+\exp\left(\frac{11.7-V}{12.9}\right)}\right]^{1/3} \tag{5}$$

$$h_{1,\infty}(V) = \frac{0.8}{1+\exp\left(\frac{27.1+V}{4.3}\right)} + \frac{0.2}{1+\exp\left(\frac{52.9+V}{10.5}\right)} \tag{6}$$

2.1.2 Shab

The inactivating conductance encoded by *Shab* has conductance $g_{\mathrm{K,Shab}} = \overline{g_{\mathrm{K,Shab}}} h m^2$. The activation gating variable, m, has the following steady-state properties:

$$m_\infty(V) = \left[\frac{1}{1+\exp\left(\frac{-1-V}{9.1}\right)}\right]^{1/2} \tag{7}$$

$$\tau_m(V) = \frac{1}{0.116\,\exp\left(\frac{-V-25.7}{32.2}\right) + 0.00659\frac{-V-23.8}{\exp\left(\frac{-V-23.8}{1.35}\right)-1}} \tag{8}$$

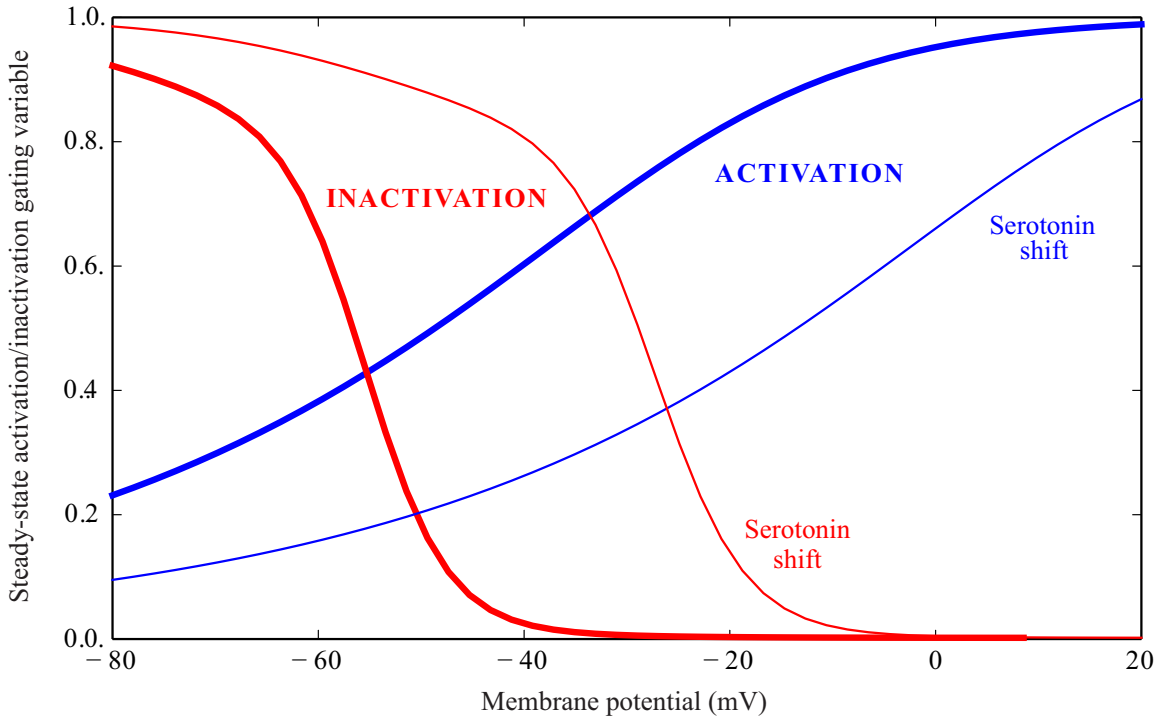

Figure 1: Steady-state activation and inactivation gating variables of Shaker in a *Drosophila* R1-6 photoreceptor. It is not shown in the figure, but note that there is also a fraction $\xi = 0.13$ of the conductance that fails to inactivate. Serotonin shifts Shaker activation and inactivation steady-state gating variables towards more depolarised potentials.

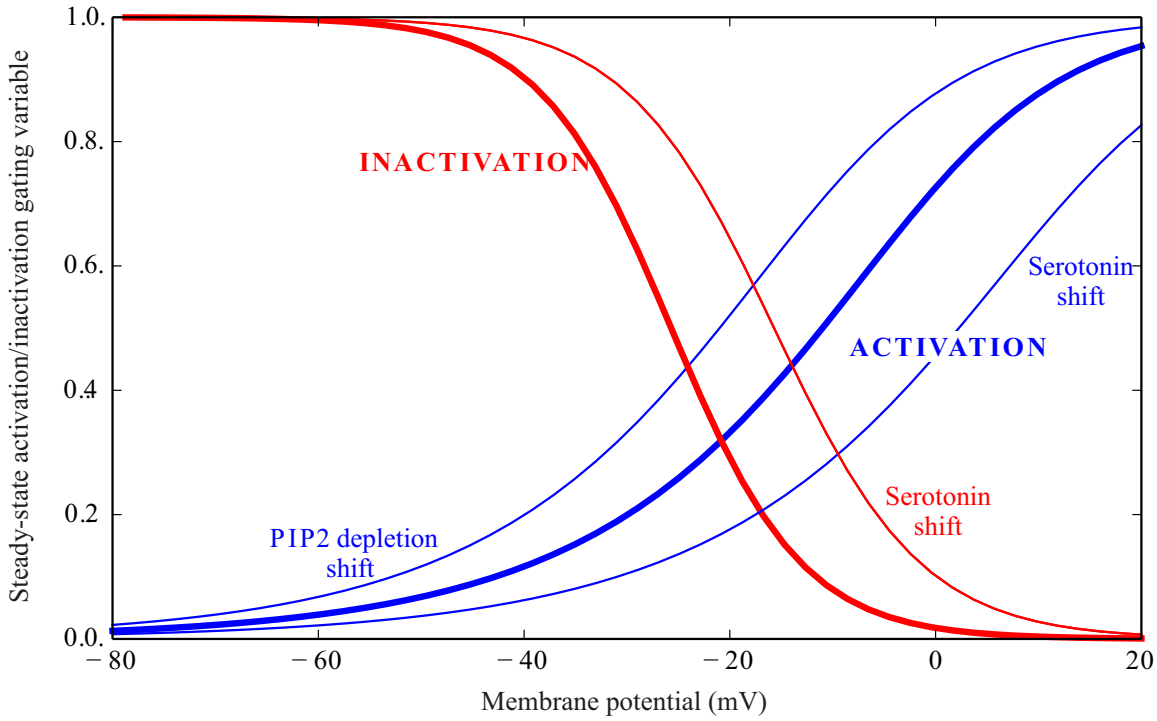

Figure 2: Steady-state activation and inactivation gating variables of Shab in a *Drosophila* R1-6 photoreceptor. Serotonin shifts Shab activation and inactivation steady-state gating variables towards more depolarised potentials, while PIP2 depletion by light shifts activation towards hyperpolarised potentials.

There are two modes of inactivation, with different kinetics, related to conformational changes produced when a K^+ ion occupies the selectivity filter of the channel (Immke et al., 1999). We modelled the inactivation as a sum of two variables representing each mode of inactivation $h = \xi h_1 + (1-\xi)h_2$. The relative importance of the fast mode is considered to be constant around $\xi = 0.7$ (Krause et al., 2008).

We modelled both inactivation components with the same steady state:

$$h_{1,\infty}(V) = h_{2,\infty}(V) = \frac{1}{1+\exp\left(\frac{25.7+V}{6.4}\right)} \tag{9}$$

but different time constants

$$\tau_{h,1} = 335\ \exp\left(\frac{V}{71.3}\right) + 73.2 \tag{10}$$

$$\tau_{h,2} = 3000 \tag{11}$$

In the presence of serotonin, the steady-state curves and time constant curves are shifted towards positive potentials: activation by 13.7 mV and inactivation by 10 mV. In addition, the steady-state curves suffer small shape changes (Figure 2):

$$m_\infty(V) = \left[\frac{1}{1+\exp\left(\frac{12.7-V}{9.5}\right)}\right]^{1/2} \tag{12}$$

$$h_{1,\infty}(V) = h_{2,\infty}(V) = \frac{1}{1+\exp\left(\frac{15.7+V}{7.2}\right)} \tag{13}$$

PIP2 depletion produces a leftward 10 mV shift in the Shab component of the conductance (Krause et al., 2008) (Figure 2). We model it as a 10 mV shift in the steady-state activation curve of Shab. Although Krause et al., 2008 found some evidence that it affects more the slow inactivation component, we will apply the same shift to both components.

2.1.3 Novel conductance

We modelled the non-inactivating K^+ conductance discovered in double shaker,shab mutants (Vähäsöyrinki et al., 2006), as $g_{\mathrm{K,Novel}} = \overline{g_{\mathrm{K,Novel}}}m$. The activation variable m has the following steady-state conductance and time constant:

$$m_\infty(V) = \left[\frac{1}{1+\exp\left(\frac{-1-V}{9.1}\right)}\right]^{1/2} \tag{14}$$

$$\tau_m(V) = 13 + 165\ \exp\left[-2\left(\frac{V+19.4}{30}\right)^2\right] \tag{15}$$

Steady-state activation variable, $m_\infty(V)$, is shown in Figure 3.

2.2 A biophysical model of the fruit fly R1-6 photoreceptor membrane

Our model of the fruit fly R1-6 photoreceptor membrane has capacitance 50 pF, intermediate among modern mesurements of 30 pF to 65 pF (Kauranen and Weckström, 2004; Vähäsöyrinki et al., 2006). It contains the three types of K^+ conductances described above, namely Shaker, Shab and the Novel conductance, plus the light induced curent (LiC). A Na^+/K^+ ATPase (Jansonius, 1990; Gerster et al., 1997) and a Na^+/Ca^{2+} exchanger (Minke and Armon, 1984; Hryshko et al., 1996; Wang et al., 2005; Chu et al., 2013; Gerster, 1997) maintain homeostasis by reversing the flux of ions. The K^+ reversal potential, E_{K}, is -85 mV, and the reversal potential of LiC is $E_{\mathrm{L}} = 5$ mV.

To reproduce a dark resting potential of -68 mV and input resistance in the dark of just below 300 MΩ (at the lower end of the *in vivo* electrophysiological experimental values, reported to be as low as a couple of hundred MOhm (Abou Tayoun et al., 2011), 410 MΩ (Niven et al., 2003b) or 1240 MΩ (Juusola and Hardie, 2001)) we included a 0.803 nS leak conductance with the reversal potential of the LiC and a 2.1 nS K^+ leak conductance. From the dark resting potential, the photoreceptor model is depolarised by increasing the LiC. The recordings of the maximum steady-state depolarisation range from -45 mV (Niven et al., 2003b) to almost -30 mV (Juusola and Hardie, 2001; Niven et al., 2007), and we chose the intermediate value of -36 mV.

2.3 Calculation of the steady state

We calculated the steady-state values of the conductances at different membrane potentials using well-known procedures. The total K^+ conductance is the sum of the K^+ voltage-dependent conductances and K^+ leak conductance.

$$g_{\mathrm{K}} = g_{\mathrm{K,Shaker}} + g_{\mathrm{K,Shab}} + g_{\mathrm{K,Novel}} + g_{\mathrm{K,leak}} \tag{16}$$

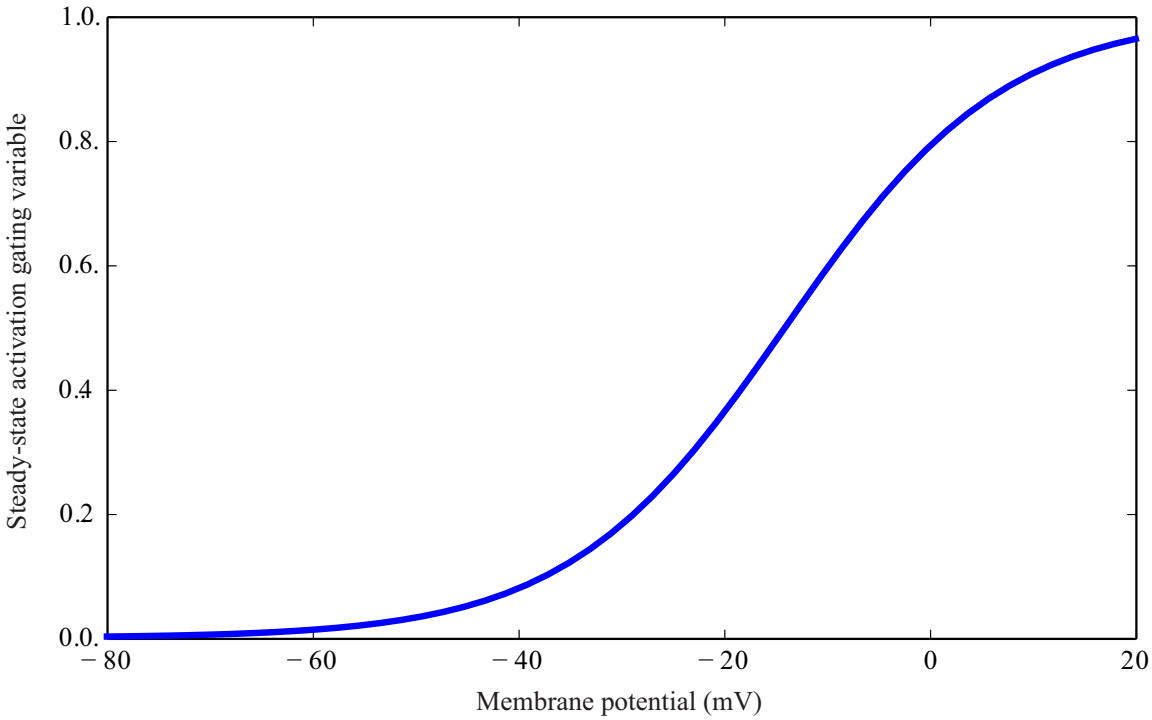

Figure 3: Steady-state activation gating variable of the Novel conductance in a *Drosophila* R1-6 photoreceptor.

and the total depolarising conductance is the sum of the current flowing trough the leak conductance and the light-induced conductance

$$g_{\mathrm{L}} = g_{\mathrm{light}} + g_{\mathrm{leak}} \tag{17}$$

We assume that the LiC is mediated by Na^+ (74%) and Ca^{2+} (26%), with a constant current fraction across voltages (Chu et al., 2013), and that only K^+ flows throught the K^+ conductances. At each steady-state depolarized membrane potential, V, we assume that all ionic currents, K^+, Na^+ and Ca^{2+}, are restored by the Na^+/K^+ ATPase and the Na^+/Ca^{2+} exchanger. In each cycle, the Na^+/K^+ ATPase pumps two K^+ ions in and three Na^+ ions out at the cost of one ATP molecule. The Na^+/Ca^{2+} exchanger interchanges one Ca^{2+} by three Na^+ ions. The net charge transported is 1 e per cycle in both the Na^+/Ca^{2+} exchanger and the Na^+/K^+ ATPase.

This produces three equations, each equation being the result of zeroing one of the net ionic currents, $I_{(\mathrm{K})}$, $I_{(\mathrm{Na})}$ and $I_{(\mathrm{Ca})}$:

$$I_{(\mathrm{K})} = g_{\mathrm{K}}(V)\,(E_{\mathrm{K}} - V) + 2I_{\mathrm{P}} = 0 \tag{18a}$$

$$I_{(\mathrm{Na})} = 0.74 g_{\mathrm{L}}\,(E_{\mathrm{L}} - V) - 3I_{\mathrm{P}} - 3I_{\mathrm{E}} = 0 \tag{18b}$$

$$I_{(\mathrm{Ca})} = 0.26 g_{\mathrm{L}}\,(E_{\mathrm{L}} - V) + 2I_{\mathrm{E}} = 0 \tag{18c}$$

where I_{P} and I_{E} are the net currents produced by the Na^+/K^+ ATPase and the Na^+/Ca^{2+} exchanger respectively. As we know the steady-state properties of the conductances, for each membrane voltage, V, we know $g_{\mathrm{K}}(V)$ and we can solve the system of linear equations to obtain g_{light}, I_{P} and I_{E}.

2.4 RrLC approximation for the calculation of the cell impedance

The response to small injected currents of a voltage-dependent K^+ conductance can be approximated by the use of its RrL circuit (Koch, 2004; Heras et al., 2016). In the case of an inactivating conductance, $g = \bar{g} m^{\gamma} h$, the RrL circuit has two phenomenological branches, and the values of the electrical elements, R, r, L, r_h and L_h are given by

$$R = \frac{1}{\bar{g}\ m^{\gamma} h} \tag{19a}$$

$$r = \frac{\alpha + \beta}{\gamma\ \bar{g}\ m^{\gamma-1} h (V - E_{\mathrm{K}})[\alpha' - m(\alpha' + \beta')]} = \frac{1}{(V - E_{\mathrm{K}})\bar{g} h \frac{\mathrm{d}}{\mathrm{d}V} m^{\gamma}} \tag{19b}$$

$$L = \frac{r}{\alpha + \beta} = \tau r \tag{19c}$$

$$r_h = \frac{\alpha_h + \beta_h}{\bar{g}\ m^{\gamma}(V - E_{\mathrm{K}})[\alpha'_h - h(\alpha'_h + \beta'_h)]} = \frac{1}{(V - E_{\mathrm{K}})\bar{g} m^{\gamma} \frac{\mathrm{d}}{\mathrm{d}V} h} \tag{19d}$$

$$L_h = \frac{r_h}{\alpha_h + \beta_h} = \tau_h r_h \tag{19e}$$

where $\alpha_h = \alpha_h(V)$, $\beta_h = \beta_h(V)$, $\tau_h = \tau_h(V)$ are respectively the activation rate, deactivation rate and time constant of the conductance of the HH inactivation variable h at the voltage V.

We then use the values of R, r, L, r_h and L_h to compute the impedance of the K^+ conductance:

$$Z_{\mathrm{c}}^{-1}(f) = \frac{1}{R} + \frac{1}{r + i2\pi f L} + \frac{1}{r_h + i2\pi f L_h} = \frac{1}{R} + \frac{1/r}{1 + i2\pi f \tau} + \frac{1/r_h}{1 + i2\pi f \tau_h} \tag{20}$$

R, r and L are positive quantities, but r_h and L_h are negative quantities. r_h and L_h can be substituted by a positive resistance r_h^* and positive capacitance C_h^* as described elsewhere (Koch, 1984). We do not do this, as we will use only those values to obtain the impedance.

If a conductance has different modes of inactivation or partial inactivation, the conductance can be divided into several conductances either non-inactivating or with only one mode of inactivation, and Equation 20 can be applied to each different component.

Once all the impedances of the different conductances, $Z_{Shaker}(f)$, $Z_{Shab}(f)$ and $Z_{\mathrm{Novel}}(f)$, have been calculated using Equation 20, the impedance of the whole photoreceptor is:

$$Z(f) = \frac{1}{Z_{Shaker}^{-1}(f) + Z_{Shab}^{-1}(f) + Z_{\mathrm{Novel}}^{-1}(f) + g_{\mathrm{K,leak}} + g_{\mathrm{L,leak}} + i2\pi f C} \tag{21}$$

where $g_{\mathrm{K,leak}}$ and $g_{\mathrm{L,leak}}$ are the two leak conductances and $i2\pi f C$ is the admittance of the membrane capacitance, C.

Note that for small deviations around the steady state, we consider I_{P} and I_{E} as fixed currents, which do not affect the photoreceptor impedance.

2.5 Voltage contrast gain

To account for the effect of voltage-dependent channels upon phototransduction gain, we implemented a simple transduction model. In this simple model, g_{light} follows light contrast, $c(t)$, without any filtering or adaptation in the range of frequencies considered:

$$g_{\mathrm{light}} = \overline{g_{\mathrm{light}}}(1 + c(t)) \tag{22}$$

where $\overline{g_{\mathrm{light}}}$ is the steady-state light induced conductance.

When the perturbations around the steady state, $\overline{g_{\mathrm{light}}}$, are small, the resulting voltage fluctuations are much smaller than $E_{\mathrm{L}} - V$, and the effect of the change in light contrast is equivalent to an injected current of zero mean:

$$I_{\mathrm{contrast}} = \overline{g_{\mathrm{light}}} c(t)(E_{\mathrm{L}} - V) \tag{23}$$

In the frequency domain, this current injected in a photoreceptor with membrane impedance $Z(f)$ produces the following voltage fluctuations:

$$V(f) = I_{\mathrm{contrast}}(f) Z(f) = \overline{g_{\mathrm{light}}} c(f)(E_{\mathrm{L}} - V) Z(f) \tag{24}$$

where, abusing the notation, we used the same symbol ($I_{\mathrm{contrast}}(f)$ and $c(f)$) than in the time domain for the Fourier transforms. From this equation, we deduce that the light contrast gain is:

$$T(f) = V(f)/c(f) = \overline{g_{\mathrm{light}}}(E_{\mathrm{L}} - V) Z(f) \tag{25}$$

In a real photoreceptor, at low frequencies, contrast gain is reduced by adaptation, and at high frequencies it is reduced by the bump finite width and latency dispersion (Wong et al., 1980; Wong et al., 1982). As a result, Equation 25 is a theoretical maximum, and will be a valid approximation only at intermediate frequencies.

2.6 Energy consumption

We obtain the net pump current solving Equations 18. Because the Na^+/K^+ ATPase hydrolyses an ATP molecule for every 2 K^+ ions pumped in and 3 Na^+ ions pumped out (Jansonius, 1990), we can calculate the pump energy consumption:

$$Cost = |I_{\mathrm{P}}|/e \tag{26}$$

in hydrolysed ATP molecules/s when the current, I_{P}, is given in amperes and the elementary charge, e, is in coulombs. This is the dominant cost of the photoreceptor (Laughlin et al., 1998).

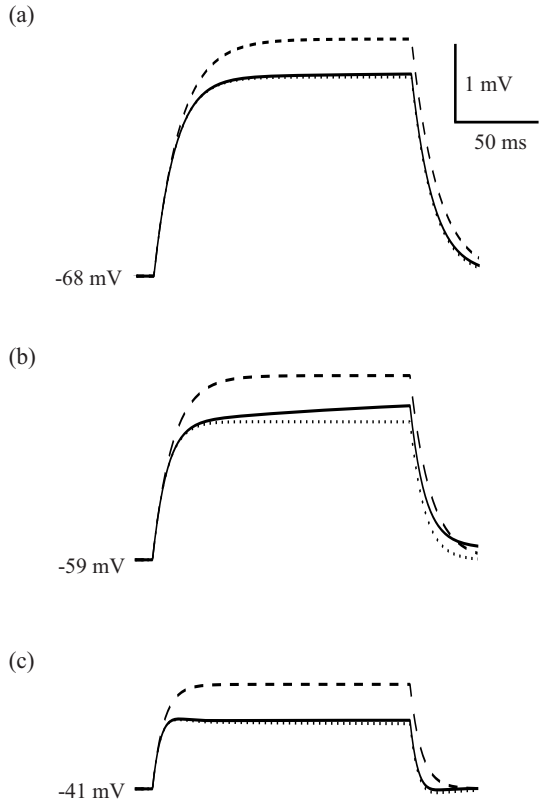

Figure 4: Voltage responses of simulated *Drosophila melanogaster* R1-6 photoreceptors to 0.01 nA injected current pulses (a) Voltage response of a dark adapted membrane. Three curves are plotted. Continuous line shows the result of a simulation where all gating variables are allowed to change following Hodkgin-Huxley equations, and thus the voltage response shows both negative and positive feedback. Dotted line is the result of a simulation where inactivation gating variables of all conductances are kept fixed in their steady-state value, and thus there is negative feedback but no positive feedback. Dashed line shows the result of keeping all gating variables (activation and inactivation) fixed during simulation, or equivalently, the voltage response of a passive membrane with the same membrane resistance and capacitance. (b) Same as (a) but in a photoreceptor that has been depolarised by light to -59 mV. (c) Same as (a) and (b) but in a photoreceptor that has been depolarised by light to -41 mV.

3 Results

We modelled the electrical properties of a fruit fly R1-6 photoreceptor membrane to explore the effects of a combination of voltage-dependent K^+ conductances on both the membrane filter properties and the photoreceptor energy consumption. We modelled the photoreceptor soma as a single electrical compartment, ignoring the effect of the axon. We implemented three types of voltage-dependent K^+ conductances: a rapidly activating and inactivating current encoded by *Shaker* (Hardie, 1991), a slowly activating and inactivating current encoded by *Shab* (Hardie, 1991; Vähäsöyrinki et al., 2006) and a very slowly activating/non-inactivating current, the "Novel" conductance (Vähäsöyrinki et al., 2006). We used a Hodgkin-Huxley (HH) framework (Hodgkin and Huxley, 1952) for the K^+ conductances, with activation and inactivation rates obtained from previous studies (Niven et al., 2003b; Kauranen and Weckström, 2004; Vähäsöyrinki et al., 2006).

3.1 Negative and positive feedback shape the voltage responses to injected current

The electrical properties of the membrane, including the voltage-dependent activation and inactivation of conductances, determine the voltage response to injected current. We simulated the voltage responses of the photoreceptor to small injected current pulses to separate the contribution of the different voltage-dependent conductances (Figure 4). We performed these simulation at different light depolarisations, obtained by increasing the light-induced conductance (LiC).

At all light depolarisations, activation of a voltage-dependent K^+ conductance performs negative feedback, while inactivation of a voltage-dependent K^+ conductance performs positive feedback. To distinguish the effects of negative and positive feedback, we freeze —i.e. we selectively keep fixed in their steady-state values— the activation and/or inactivation gating variables. When the inactivation gating variables are frozen positive feedback disappears. When all gating variables are frozen both positive and negative feedback disappear, and the voltage response reverts to the RC charging curve of a passive membrane.

The voltage responses of photoreceptors with active membranes (henceforth referred to as active photoreceptors) initially follow the RC charging curve of the passive photoreceptor (Figure 4) but diverge after a few milliseconds

the negative feedback because activation reduces the voltage deflection. Conductance inactivation is slower than activation, so the positive feedback produced from inactivation appears later than the negative feedback produced by activation.

The dark adapted photoreceptor produces the largest voltage responses to injected current (Figure 4a) because there is little activation of voltage-dependent conductances at -68 mV. There is, however, some negative feedback due to the fast activation of Shaker and the comparatively slower activation of Shab, reducing the voltage signal of the active photoreceptor below that of the passive photoreceptor by about 15%. After a couple of tens of milliseconds, Shaker inactivation produces a small amplification (approximately 1.5% after 150 ms).

Increasing the light induced conductance, as occurs in low light intensities, depolarizes the simulated photoreceptor to -59 mV. The membrane resistance decreases because of the increased light-induced and K^+ conductances. As a consequence, the voltage responses become smaller (Figure 4b). Negative feedback becomes more apparent, subtracting approximately 25% from the voltage response, whilst positive feedback due to Shaker fast inactivation amplifies the depolarisation by approximately 9% at the end of a 150 ms pulse (Figure 4b), and up to 15% in longer pulses (not shown).

At high light levels, when the light-induced conductance depolarizes the model photoreceptor to -41 mV, the membrane resistance is further decreased and the voltage responses become smaller (Figure 4c). Negative feedback due to conductance activation becomes conspicuous decreasing gain by approximately 37%, and producing an overshoot and an after-potential. Positive feedback due to conductance inactivation is reduced (less than 4% after a 150 ms pulse). At the end of the 150 ms pulse, about 20% of the positive feedback is due to Shab inactivation (not shown). This positive feedback is more apparent in longer time scales because of the slow dynamics of Shab inactivation, when it is responsible of about one third of the total inactivation (not shown).

3.2 Negative and positive feedback shape the membrane impedance

To analyse the contribution of the voltage-dependent conductances to the membrane's frequency response, we calculated the impedance, $Z(f)$, which determines the linear filtering characteristics of the membrane in the frequency domain. By solving an RrLC electrical circuit that represents the linearization of the membrane incorporating voltage-dependent conductances, we obtained a closed formula that allowed us to calculate the impedance (see Material and methods) (Koch, 1984; Heras et al., 2016). Using this closed formula, we calculated the impedance at each light level, depolarising the photoreceptor by increasing the light conductance.

In the dark, the membrane is a low-pass filter (Figure 5a), not very different from an RC filter with the same resistance and impedance. The feedback produced by voltage-dependent conductances lowers the impedance of the active membrane at every frequency to below that of the passive membrane with the same membrane resistance and capacitance. At low light levels, when the photoreceptor is depolarized to between -59 mV and -50 mV, the impedance shows a conspicuous low frequency amplification below 2-3 Hz (Figure 5a) that corresponds to the positive feedback due to Shaker inactivation. This amplification is produced solely by positive feedback from Shaker inactivation, and does not depend on a window current as previously suggested (Niven et al., 2003b). At high light levels the photoreceptor is depolarized to above -41 mV, the negative feedback causes the impedance to become band-passing, and the Shaker-mediated amplification disappears (Figure 5a). Only at the highest light levels does the positive feedback from Shab inactivation amplify frequencies below 1 Hz. At medium and high light levels, the Novel conductance produces negative feedback that decreases impedance at low frequencies diminishing the low frequency amplification of Shab.

3.3 Negative feedback reduces the cost of membrane bandwidth and increases the gain-bandwidth product

The membrane bandwidth determines the range of frequencies across which the photoreceptor can respond. At low frequencies, other slower adaptation processes affect the frequency response decreasing amplification, as suggested by the lack of significant linear amplification in the light response (Juusola et al., 2003). This suggests that amplification below 2 Hz may not be the primary function of the Shaker conductance and is merely a side effect of the relatively slow inactivation of fruit fly voltage-dependent conductances. Thus, we restrict our definition of bandwidth to frequencies above 2 Hz. The photoreceptor membrane increases its bandwidth from around 26 Hz in the dark adapted state to more than 100 Hz at the highest light levels (Figure 5d).

Photoreceptor energy consumption at each depolarisation level can be calculated from the flux of Na^+ and K^+ ions across the membrane, which must be pumped back across to the opposite side by the Na^+/K^+ pump (see Methods). The 4-fold increase in photoreceptor bandwidth from the lowest to the highest light levels is produced at the cost of a 4.3-fold increase in energy consumption, from 1.3×10^8 ATP/s in the dark to 5.6×10^8 ATP/s at the highest light levels (Figure 5e).

At all light levels, the conductance properties boost the bandwidth of the photoreceptor membrane above that of a passive membrane with identical resistance and capacitance (Figure 5d). In the dark, the active photoreceptor membrane has a 6 Hz higher bandwidth than the corresponding passive membrane, increasing to 10 Hz at low light levels. At the highest light levels, the active photoreceptor membrane has a 40 Hz higher bandwidth than the corresponding passive membrane, an improvement of more than 70%. To achieve the same bandwidth as the active

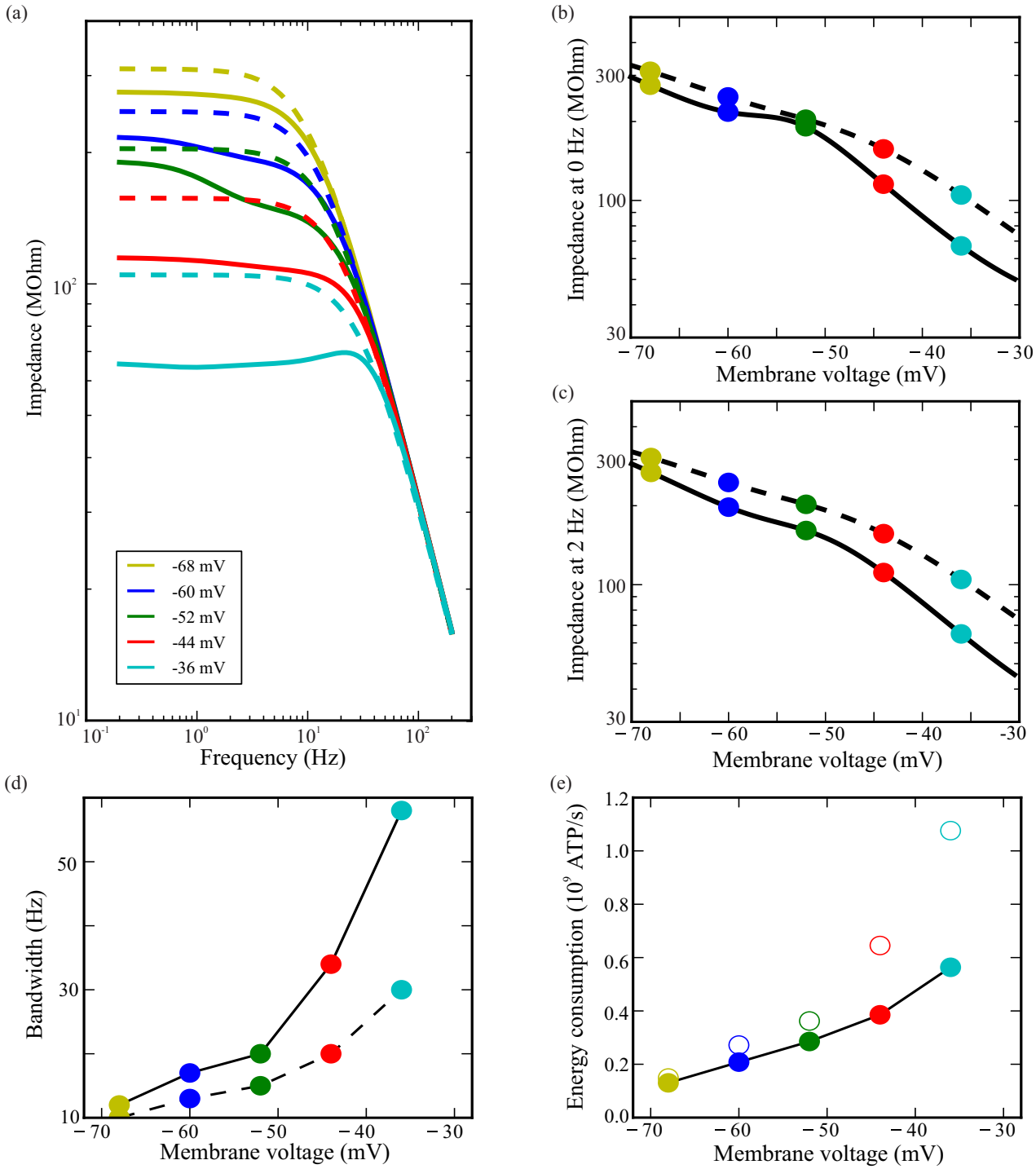

Figure 5: The effects of feedback produced by K^+ conductances on a model photoreceptor, at dark resting potential and depolarised by light-induced current to four steady-state membrane potentials (a) Photoreceptor impedance in simulated photoreceptors depolarised by light to different voltages (solid lines). Dashed lines represent the membrane impedances of photoreceptors with frozen conductances, i.e. where the activation and inactivation gating variables are kept constant at each steady state when computing the impedance. They are RC membranes with the photoreceptor capacitance and true membrane capacitance fixed at the value taken in that particular voltage. The low frequency limits and values of the impedance at 2 Hz are represented in subfigures (b) and (c). (d) The bandwidth of simulated photoreceptors with active K^+ conductances (solid line) depolarised by light to different voltages versus the bandwidth of photoreceptors with frozen conductances at each voltage (dashed line). (e) Photoreceptor energy consumption increases with depolarisation. At each depolarisation, the cost of an active fruit-fly photoreceptor (filled circles) is smaller than that of a passive photoreceptor with the same bandwidth and capacitance (empty circles).

photoreceptor membrane with a passive membrane would increase the energy cost by 10% at low light levels rising to 40% at high light levels (Figure 5e).

3.4 Negative feedback increases the gain-bandwidth product (GBWP)

Using the active and passive membrane impedances, we calculated the gain-bandwidth product (GBWP), the product of bandwidth and peak impedance (Heras et al., 2016). The GBWP of the active photoreceptor membrane generally increases with depolarisation, though there is a pronounced 'dip' at intermediate voltages around -52 mV (Figure 6). In contrast, the GBWP of the corresponding passive membranes remains constant. The increase in GBWP in the active photoreceptor is produced by feedback from the voltage-dependent K^+ conductances. The inductive effects of these conductances produce shunt peaking, which increases the GBWP (Heras et al., 2016). At low light levels this increase is 10-15%, increasing to 25% at the highest light levels.

By selectively freezing the gating variables of the different voltage-dependent conductances, we distinguished the contributions of each conductance to shunt peaking (Figure 6). Shaker activation is the major contributor to shunt peaking at low light levels (membrane voltages below $-55\,\mathrm{mV}$). At higher light levels, however, Shab activation becomes the major contributor to shunt peaking. Activation of the Novel conductance is too slow to significantly contribute to shunt peaking at any light level.

3.5 Inactivation of voltage-dependent K^+ conductances affects photoreceptor bandwidth and energy consumption

The voltage-dependent Shaker and, to a lesser extent, the Shab conductances in Drosophila R1-6 photoreceptors inactivate. To assess the role of inactivation in these voltage-dependent K^+ conductances, we froze the inactivation variable at different light levels, and assessed the bandwidth and energy consumption of these photoreceptor membranes across the full operating range of the photoreceptor (Figure 7). All other features of the photoreceptors remained identical. At low light levels, close to the resting potential there is little inactivation of the voltage-dependent K^+ conductances. Membranes with inactivation frozen at these low light levels have a similar bandwidth and energy consumption to typical photoreceptors. As light levels increase and the photoreceptor depolarises, however, the bandwidth and energy consumption of these membranes is substantially higher than that of a typical photoreceptor (Figure 7a and b).

When inactivation is frozen at high membrane potentials that correspond to high light levels, photoreceptor bandwidth and energy consumption is unaffected at high and at mid light levels (Figure 7a and b). Conversely, at low light levels these membranes have lower energy cost but also lower bandwidth. The increase in bandwidth at low light levels is small in absolute terms but is relatively large. There is almost no change in the energy cost of bandwidth itself, so energy savings are made not through increased energy efficiency but rather by reducing bandwidth at high light levels (Figure 7c). Thus, inactivation of a voltage-dependent K^+ conductance allows relatively high bandwidths and energy costs at low light levels but ensures that there is no corresponding increase in bandwidth and energy costs at high light levels.

3.6 Feedback decreases photoreceptor voltage gain and decreases the cost of phototransduction gain-bandwidth product

Photoreceptor contrast gain depends not only on the membrane impedance but also on the light-induced current (LiC). To determine how the membrane filter properties affect photoreceptor contrast gain, we incorporated a simplified, infinitely fast phototransduction cascade (Equations 22, 23). The voltage contrast gain is then the product of the LiC and membrane impedance (Equation 25).

Feedback from the voltage-dependent K^+ conductances changes the impedance but does not change the LiC. Consequently, negative feedback from activation decreases the voltage contrast gain of an active photoreceptor compared to that of a passive photoreceptor with identical membrane resistance and capacitance (Figure 8a). The net consequence is that, in our model, voltage-dependent conductances decrease the photoreceptor peak voltage contrast gain (i.e. the maximum of voltage contrast gain across different frequencies) at all light intensities.

The contrast gain-bandwidth product (cGBWP) is the product of the bandwidth and the peak voltage contrast gain. In our simplified model, the voltage contrast gain is the product between light induced current and membrane impedance (Equation 25), so the cGBWP is the product of GBWP and LiC. Consequently, the cGBWP of the active membrane exceeds that of the passive membrane by 10-15% at low light levels increasing to 25% at high light levels (Figure 8b).

3.7 Light Dependent Modulation (LDM) of voltage-dependent K^+ conductances change membrane impedance, gain and energy consumption

A light-dependent modulation (LDM) has been described in *Drosophila* R1-6 photoreceptors, arising from the action of PIP2 upon microvillar-bound Shab channels, which shifts their activation $10\,\mathrm{mV}$ towards negative potentials (Krause et al., 2008). To determine the effect of the LDM at different depolarisations, we kept the leak and light

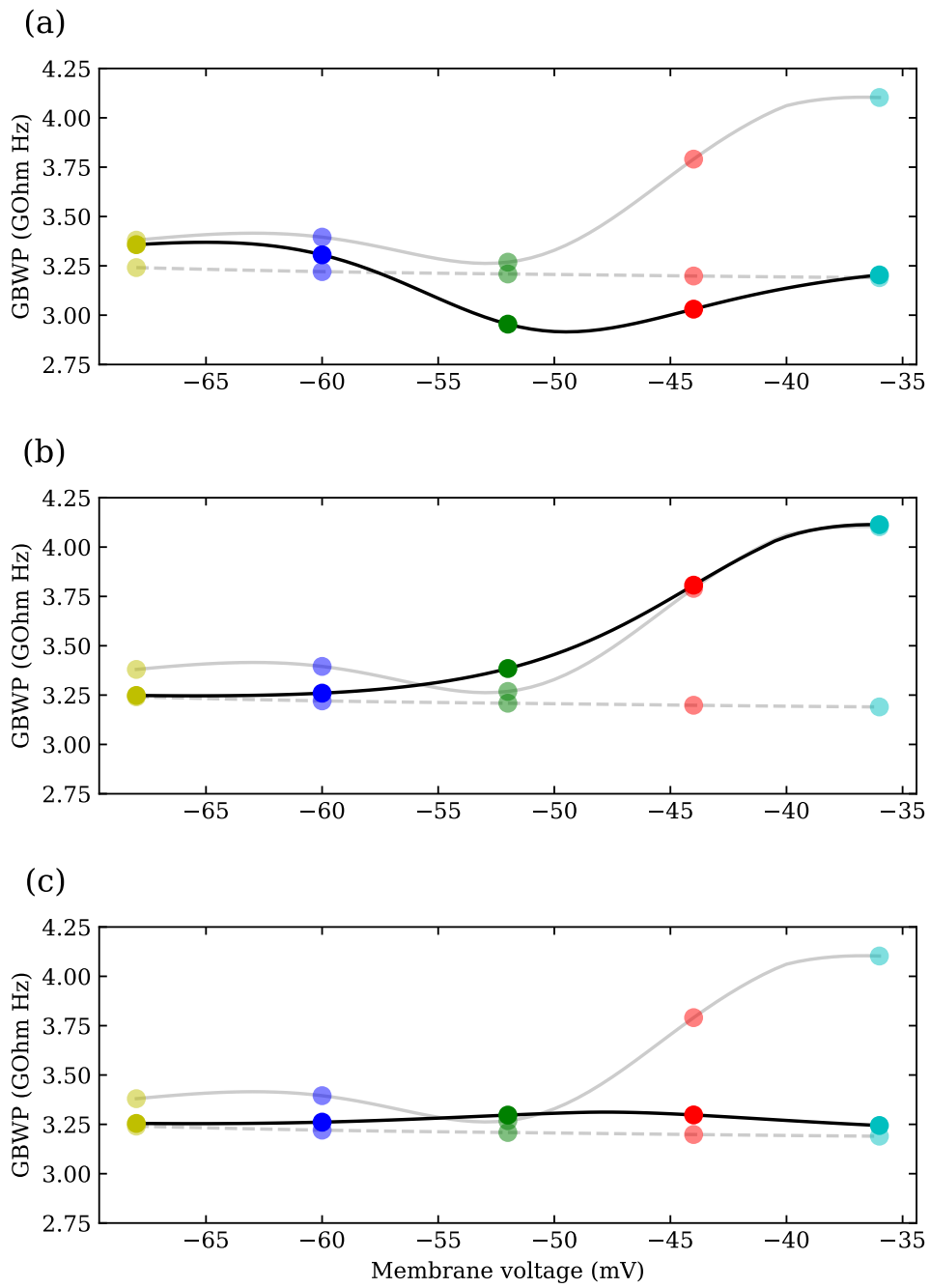

Figure 6: The contributions of the three voltage-dependent K^+ conductances to the gain-bandwidth product (GBWP) of the photoreceptor membrane, over the range of depolarisation produced by the light induced current. (a) GBWP of a fruit fly model photoreceptor across different light levels. Circles joined with black solid lines result from a model where only Shaker activation and inactivation gating variables are active, while the other two conductances are frozen, i.e. kept constant at each steady state when computing the impedance. Circles joined with grey solid lines are the result of the model with all active conductances, and circles joined with dashed lines are GBWP of the passive membrane, i.e. when all gating variables are frozen. (b) Same as (a) but keeping Shab activation and inactivation gating variables active, and freezing those of Shaker and Novel. (c) Same as (a) but keeping the Novel activation gating variable active, and freezing those of Shaker and Novel.

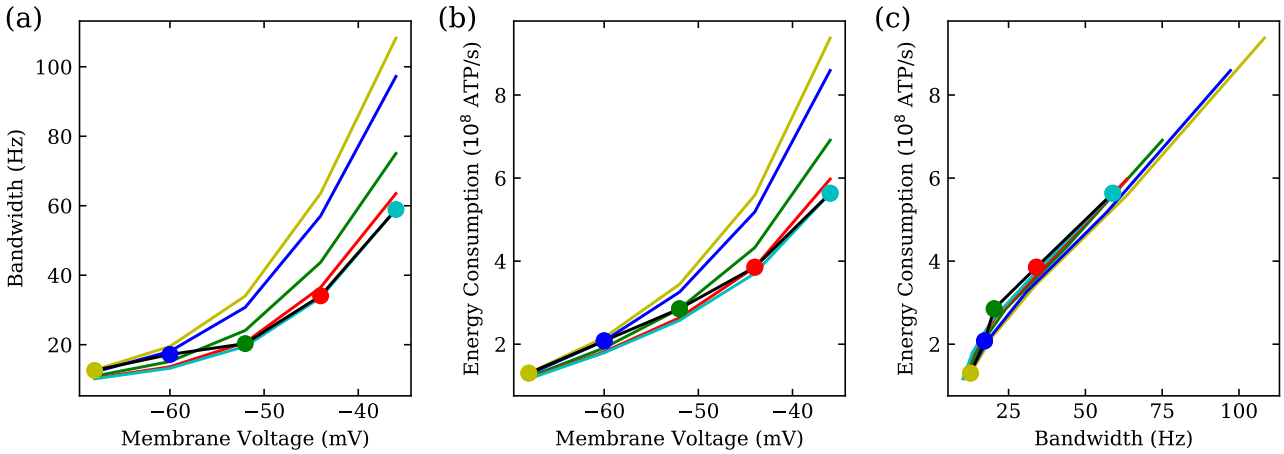

Figure 7: Inactivation of the voltage-dependent K^+ conductances affects the bandwidth and energy consumption of photoreceptors. (a) Bandwidth at different membrane voltages of the photoreceptor (black line with colour circles) compared to that of photoreceptors where inactivation of the voltage-dependent conductances has been frozen, i.e. kept constant at the value corresponding to the circle of the same color. (b) Same as (a), but plotting energy consumption against membrane voltage. (c) Same as (a), but plotting energy consumption against bandwidth.

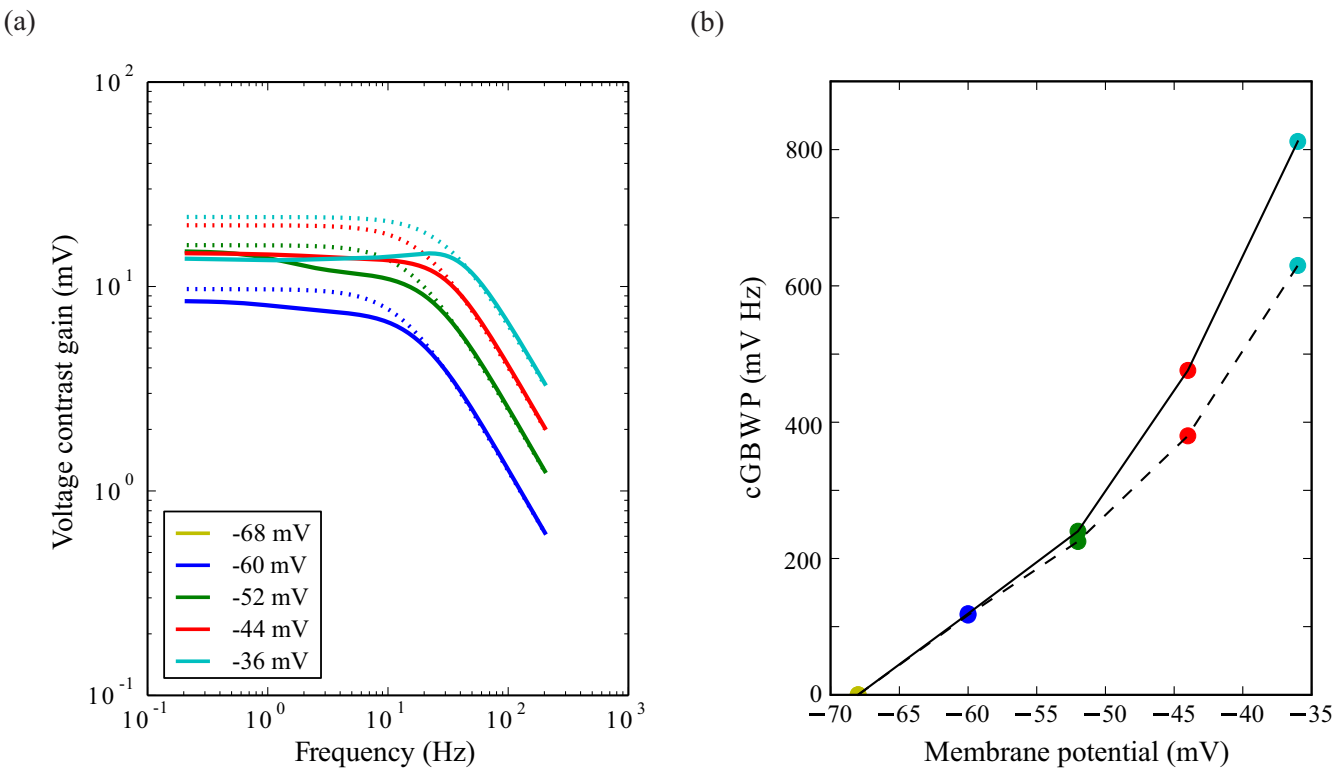

Figure 8: Voltage-dependent K^+ conductances reduce voltage contrast gain and increase contrast-gain-bandwidth product (cGBWP). (a) Voltage contrast gain of the active photoreceptors (solid line) compared to the voltage contrast gain of passive photoreceptors with the same resistance, depolarising leak conductance and capacitance (dotted line). Photoreceptors depolarised by light-induced current (LiC) to steady-state values of membrane potential indicated by coloured points in (b). Voltage contrast gain for the completely dark adapted photoreceptor does not appear in the log-log plot as it is 0 mV. (b) cGBWP of the active photoreceptors (solid line) compared to the cGBWP of passive photoreceptors with the same resistance, depolarising leak conductance and capacitance (coloured points joined with dashed line).

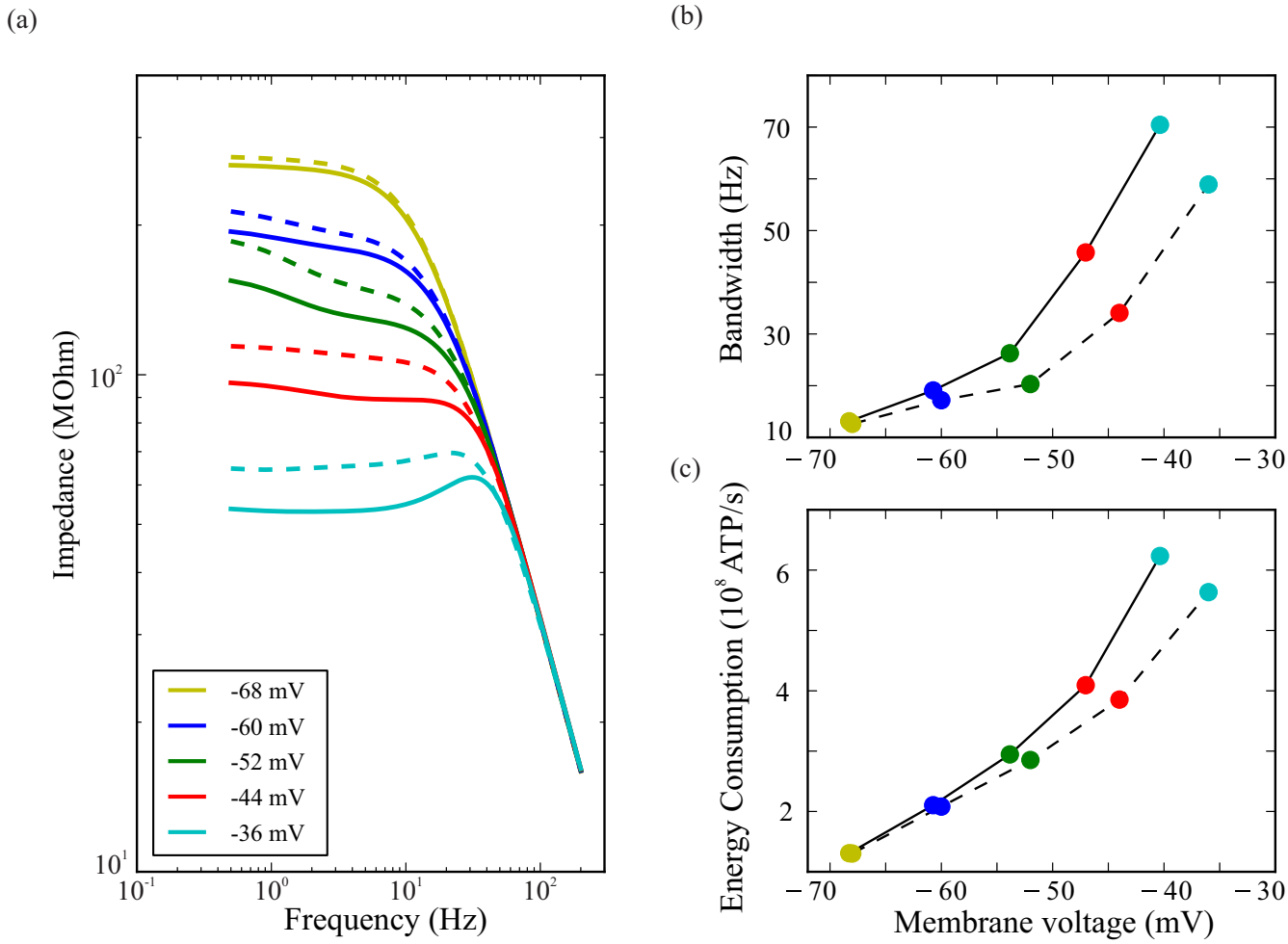

Figure 9: When PIP2 depletion shifts the voltage activation ranges of Shab, membrane impedance decreases, and bandwidth and energy costs increase. (a) Impedance with (solid lines) and without (dashed lines) the action of PIP2 depletion at four levels of depolarisation produced by changing the LiC. Dashed lines are the same as continuous lines in Figure 5a. (b) Bandwidth with (solid) and without (dashed) the action of PIP2 depletion. LiC fixed to values producing levels of depolarisation indicated by the key in (a). The leftward shift of coloured points indicates that PIP2 depletion hyperpolarises the membrane at rest, and at the 4 levels of LiC. (c) Energy cost, calculated as the rate of consumption of ATP, with (solid) and without (dashed) the action of PIP2 depletion on Shab.

conductances unchanged, allowing the membrane potential to change to a new steady-state value. The Na^+/K^+ pump and Na^+/Ca^{2+} exchanger current change accordingly.

The shift in Shab voltage-activation range produced by PIP2 depletion hyperpolarises the photoreceptor and decreases the membrane impedance (Figure 9a). Consequently, the LDM speeds up responses by widening membrane bandwidth (Figure 9) (Krause et al., 2008), and causes the effects of Shaker become less conspicuous. The increase in bandwidth is small at low light levels becoming more pronounced at higher light intensities, when the membrane potential is above −55 mV and the Shab current is larger. The Shab mediated band-passing at high light intensities becomes more prominent, and bandwidth increases by up to 18 Hz (Figure 9b). As well as increasing bandwidth, LDM affects photoreceptor energy consumption. At low light levels, LDM has little effect upon photoreceptor energy consumption but at high light intensities energy consumption is increased by as much as ∼10% (Figure 9c).

Ca^{2+} activated calmodulin modulates the maximum conductance of Shab (Peretz et al., 1998). A decrease of 50% in the maximum Shab conductance hyperpolarises the photoreceptor and increases impedance, reducing the effect of Shab mediated band-passing at the highest light levels and reducing bandwidth by up to ∼20% (not shown). It also increases gain by ∼15% and decreases energy cost by up to ∼10%. Conversely, an increase of Shab maximum conductance, the expected effect of an increase in Ca^{2+}/calmodulin upon light adaptation, has the opposite effect (not shown).

3.8 Serotinergic modulation of voltage-dependent K^+ conductances change membrane impedance, gain and energy consumption

Serotonin (5HT) reversibly shifts the activation and inactivation curves of the Shab conductance by ∼30 mV and the activation and inactivation curves of the Shaker conductance by 10 to 14 mV (Hevers and Hardie, 1995). The higher activation voltages of the shifted K^+ conductances caused by serotonin depolarises photoreceptors slightly

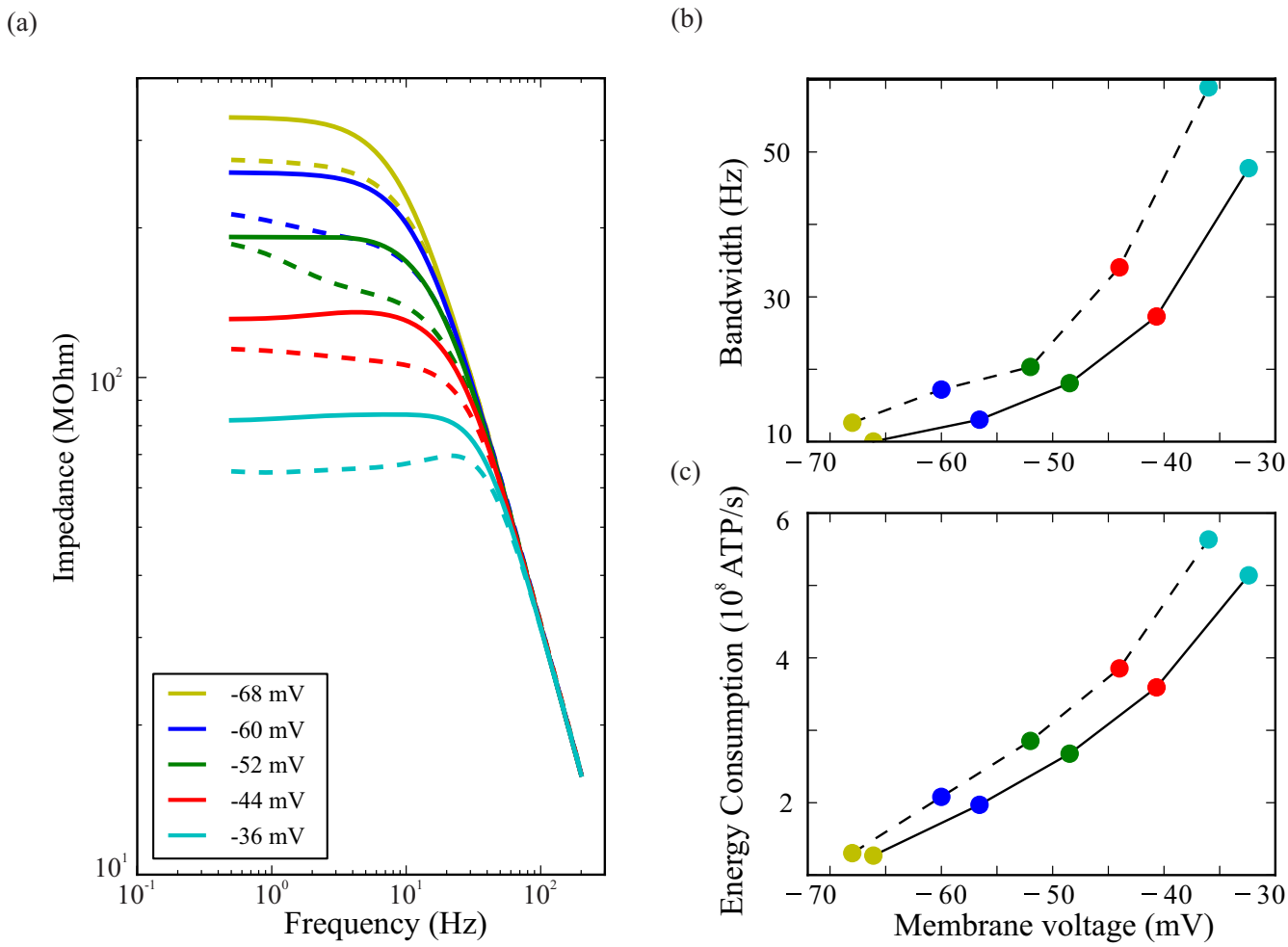

Figure 10: When serotonin shifts the voltage activation ranges of Shaker and Shab, membrane impedance increases, and bandwidth and energy costs decrease. (a) Impedance with (solid curves) and without (dashed curves) the action of serotonin at four levels of depolarisation produced by fixing the LiC. (b) Bandwidth with (solid) and without (dashed) the action of serotonin. LiC fixed to values producing levels of depolarisation indicated by the key in (a). The rightward shift of coloured points indicates that serotonin depolarises the membrane at rest, and at the 4 levels of LiC. (c) Energy cost, calculated as the rate of consumption of ATP, with (solid) and without (dashed) the action of serotonin on Shaker and Shab.

and alters their filter properties (Figure 10). At each light-induced level of depolarisation photoreceptor impedance increases (Figure 10a) (Kauranen and Weckström, 2004). Serotonin also abolishes Shaker-mediated amplification by shifting inactivation (Kauranen and Weckström, 2004). Consistent with the reduction in the negative feedback contributed by Shab, serotonin decreases bandwidth at all depolarisations (Figure 10b), and by as much as 40% at high light levels. By modulating the properties of the Shab and Shaker conductances, serotonin also decreases energy consumption at all light levels by as much as ∼40% (Figure 10c).

3.9 Modulation of voltage-dependent K^+ conductances adjusts the GBWP

By altering the voltage-dependent K^+ conductances, modulation can adjust the gain-bandwidth product (GBWP) of the active photoreceptor membranes. Because the effects of modulation are specific, so too are the effects on shunt peaking and, consequently, the GBWP. Light-dependent modulation (LDM) has little effect at low and high light levels (-60 and -36 mV, respectively) but increases the GBWP at intermediate light levels (-52 to -44 mV) in comparison to the unmodulated active photoreceptor membrane (Figure 11a). The increase in GBWP is a consequence of LDM inducing a 10 mV negative shift in Shab activation so that it occurs at intermediate light levels producing shunt peaking, which extends bandwidth and increases the GBWP. Reduction of the Shab conductance by 50%, as produced by Ca^{2+} activated calmodulin modulation, reduces the photoreceptor GBWP at high light levels (-44 to -36 mV) but has no substantial effect at low and intermediate light levels (Figure 11b). The reduction in GBWP at high light levels is a consequence of the smaller Shab conductance, which reduces the shunt peaking produced by Shab activation and, consequently, the GBWP. Serotonin also reduces the GBWP at high light levels but additionally reduces the GBWP at low light levels and abolishes the 'dip' at intermediate voltages (-52 mV) producing a monotonic increase GBWP with depolarisation (Figure 11c). The effects on GBWP at low and intermediate light levels are due to the positive shift in the Shaker conductance caused by serotonin; Shaker activation at intermediate light levels causes shunt peaking that increases the GBWP, and simultaneously removes shunt peaking at low light levels. The positive shift in Shab conductance by serotonin reduces shunt peaking produced by Shab, thereby reducing the GBWP at high light levels.

3.10 Modulation of voltage-dependent K^+ conductances trades-off gain for bandwidth but has little effect on the contrast gain bandwidth product (cGBWP) cost

The changes in photoreceptor membrane gain and bandwidth wrought by the modulation of voltage-dependent K^+ conductances have implications for contrast coding. Light-dependent modulation (LDM) of the Shab conductance reduces photoreceptor contrast gain below the corner frequency at all light levels (Figure 12a), increasing photoreceptor bandwidth (Figure 13a). At the highest light levels, LDM enhances the bandpassing of the membrane. Conversely, serotonergic modulation of the Shab and Shaker conductances increases photoreceptor contrast gain below the corner frequency at all light levels (Figure 12b), decreasing photoreceptor bandwidth (Figure 13a). At the highest light levels, serotonin modulation removes the bandpassing of the membrane entirely.

To quantify the impact of modulation on the trade-off between contrast gain for bandwidth, we calculated the peak voltage contrast gain and bandwidth at each light level (Figure 13). The dark adapted photoreceptor membrane has a low peak voltage contrast gain and low bandwidth. At low light levels, peak voltage contrast gain rises markedly though there is almost no change in bandwidth. At intermediate light levels, peak voltage contrast gain rises further accompanied by a substantial increase in bandwidth, whilst at the highest light levels there is almost no change in peak voltage contrast gain but bandwidth nearly doubles. Light-dependent modulation (LDM) shifts the relationship between peak voltage contrast gain and bandwidth to higher bandwidths at an equivalent peak voltage contrast gain. Conversely, serotonin modulation shifts the relationship between peak voltage contrast gain and bandwidth to lower bandwidths at an equivalent peak voltage contrast gain. Thus, modulation of the photoreceptor membrane is capable of trading-off contrast gain for bandwidth (Figure 14a).

By altering photoreceptor energy consumption, modulation also alters the energy cost of bandwidth and of peak voltage contrast gain. As light level increases, so too does bandwidth and energy cost. The energy cost of the peak voltage contrast gain follows a similar relationship to that of bandwidth and peak voltage contrast gain. Light-dependent modulation (LDM) reduces the energy cost of bandwidth but increases that of contrast gain (Figures 13b, 13c). Conversely, serotonin increases the energy cost of bandwidth and decreases that of contrast gain (Figures 13b, 13c). Thus, modulation adjusts the energy cost of peak voltage contrast gain and bandwidth.

4 Discussion

Our aim was to determine the impact of neuromodulators upon the energy efficiency of neural coding. To this end, we used a combination of computational and analytical models of the fruit fly R1-6 photoreceptor membrane that incorporate those voltage-dependent K^+ conductances present in the soma. Our analysis demonstrated that the voltage-dependent K^+ conductances fulfil previously unknown roles in photoreceptor coding, extending bandwidth, increasing the GBWP and improving energy efficiency. Using these models, we assessed the effect that changes in the voltage-dependent K^+ conductances produced by the action of neuromodulators have upon membrane filtering, signalling and energy efficiency. We show that neuromodulators trade-off contrast gain for bandwidth but do

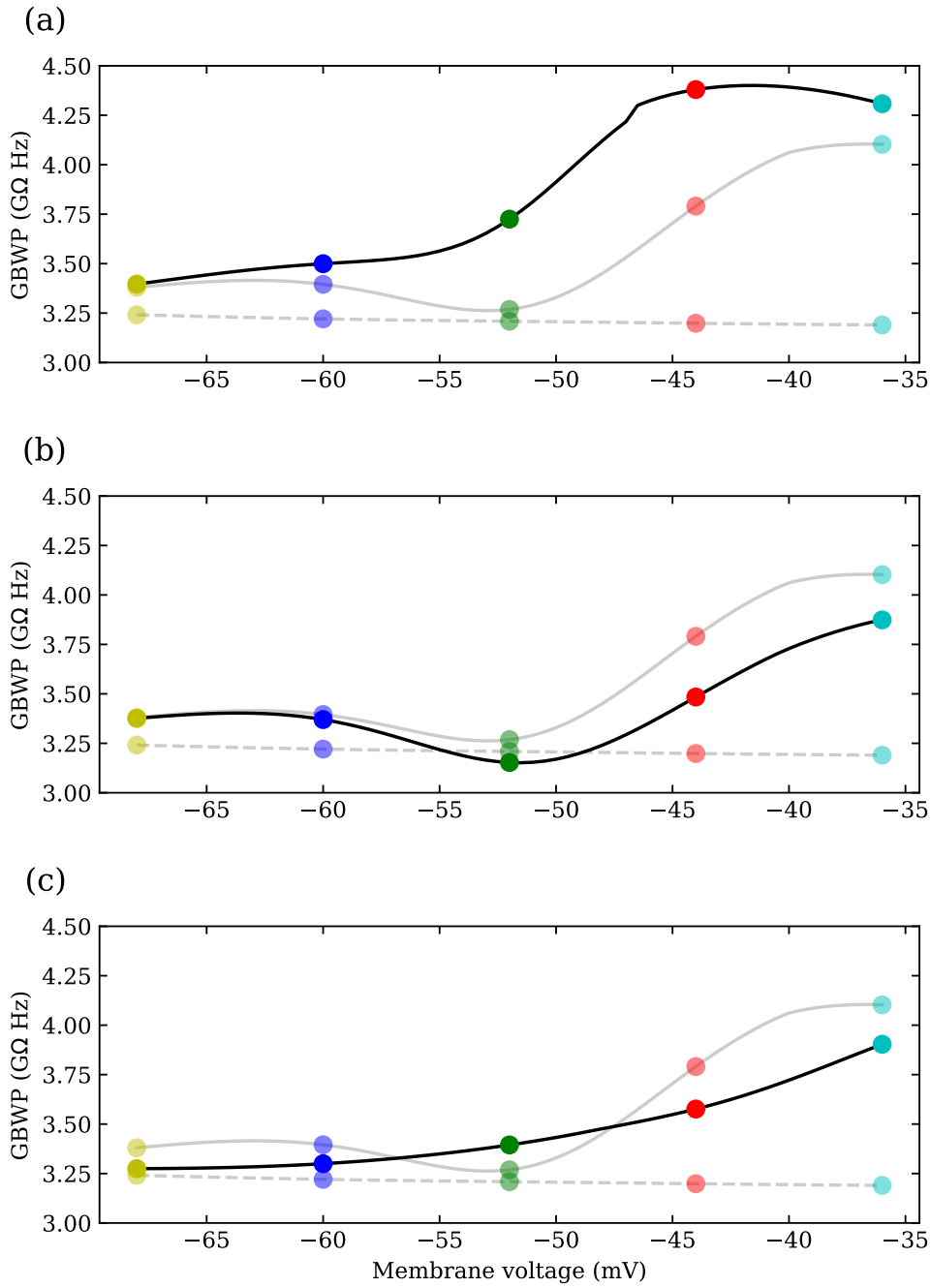

Figure 11: The contributions of different modulations to the gain-bandwidth product (GBWP) of the photoreceptor membrane, over the range of depolarisation produced by the light induced current. (a) Circles joined with black solid lines result from a model where Shab and Shaker have been modulated by PIP2 depletion. Circles joined with grey solid lines are the GBWP of the unmodulated photoreceptors, and circles joined with dashed lines are GBWP of the passive membrane, i.e. when all gating variables are frozen. (b) Same as (a) but reducing Shab conductance by 50%. (c) Same as (a) but with serotonin shifting Shaker and Shab activation and inactivation curves.

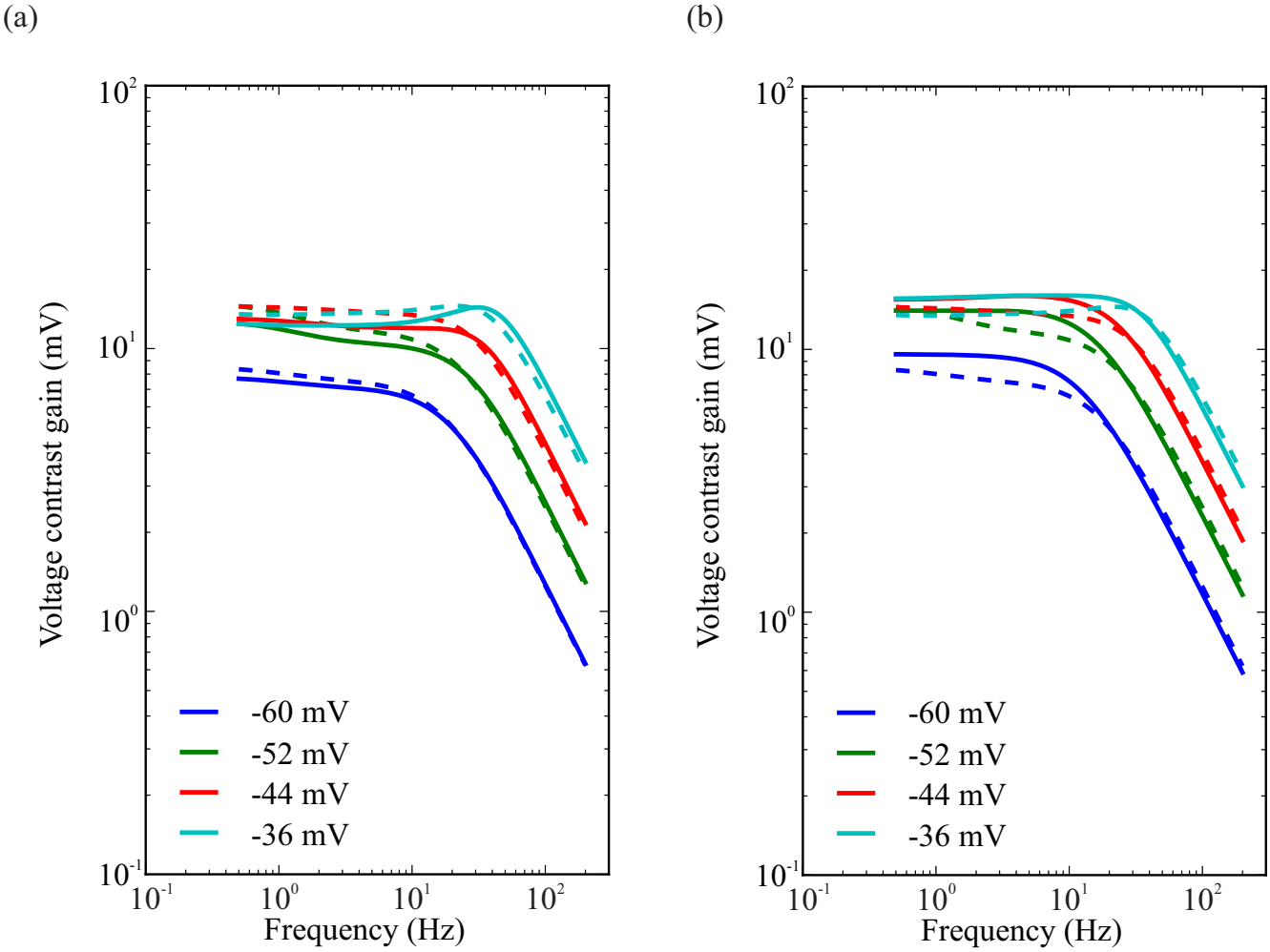

Figure 12: Voltage contrast gain with (solid curves) and without (dashed curves) the modulator shift at four levels of depolarisation. (a) Light-dependent modulation (b) Serotonin.

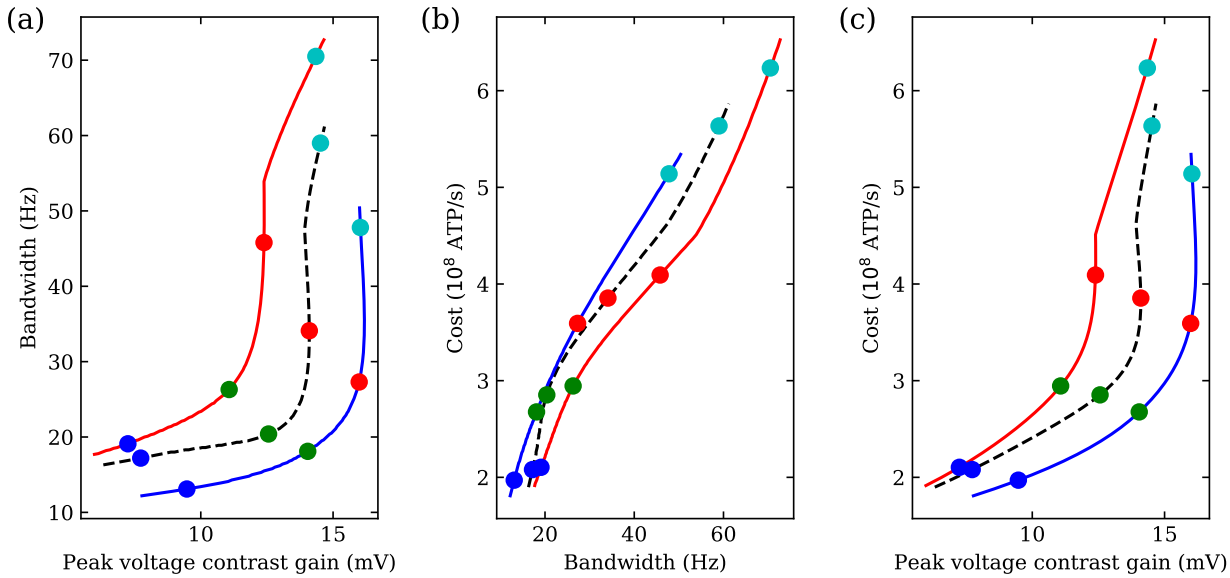

Figure 13: Modulators shift bandwidth, peak voltage contrast gain and energy consumption of photoreceptors (a) Bandwidth and voltage contrast gain plotted against each other with (solid curves) and without (dashed curves) modulation at four levels of depolarisation produced by fixing the LiC. (b) Energy consumption and bandwidth plotted against each other with (solid curves) and without (dashed curves) modulation at four levels of depolarisation produced by fixing the LiC. (c) Energy consumption and peak voltage contrast gain plotted against each other with (solid curves) and without (dashed curves) modulation at four levels of depolarisation produced by fixing the LiC.

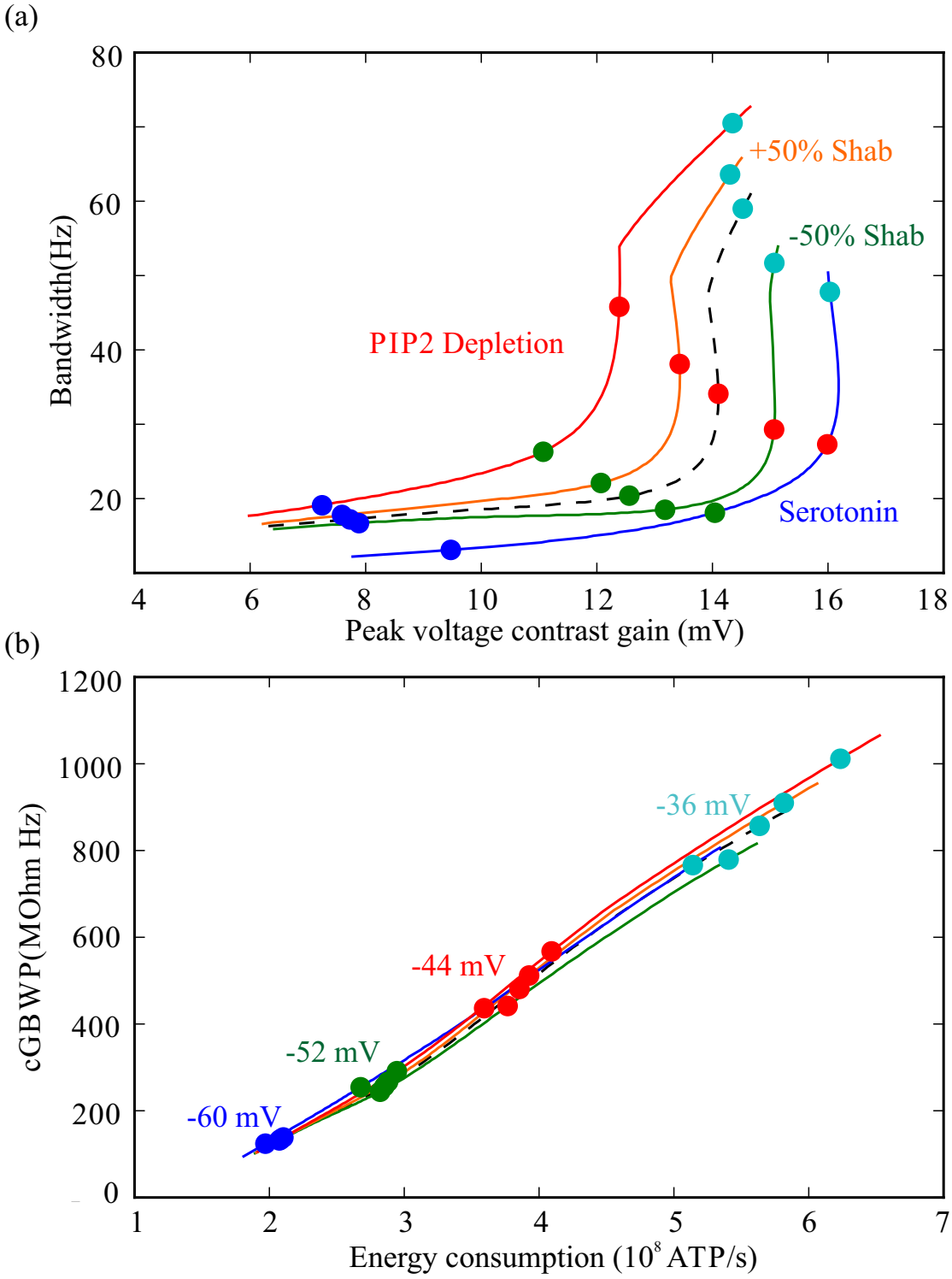

Figure 14: Shifts in voltage-dependent K^+ conductances produced by modulators trade-off gain and bandwidth but have little influence on the cost of the contrast-gain-bandwidth product (cGBWP). (a) Bandwidth and peak voltage contrast gain for the model photoreceptor with unshifted conductances (dashed black line) where LiC has been increased to depolarise to four membrane potentials (colour circles). For each depolarisation, I modified the properties of the conductances, which keeping LiC constant, and allowed the photoreceptor to reach a new depolarisation (colour circles on colour lines). (b) The original (black dashed line) and shifted (coloured lines, colour code as in (a)) photoreceptors occupy a similar space in a cGBWP vs energy cost graph, illustrating that modulators changing channel properties have little effect in the cost of cGBWP.

so without producing a substantial change in energy consumption, so that the energy cost of cGBWP remains unchanged (Figure 14b). Instead, modulation acts to adjust the energy investment in contrast gain versus bandwidth whilst maintaining the relationship between cost and cGBWP.

4.1 Voltage-dependent K^+ conductances generate negative feedback and shunt peaking that extend bandwidth and reduce cost

We began by assessing the impact of voltage-dependent K^+ conductances themselves upon the graded electrical signalling and energy consumption of fruit fly photoreceptor membranes. By activating upon depolarisation, the Shaker, Shab and Novel conductances produce negative feedback. The main role of this feedback is to reduce the impedance to below that of a passive photoreceptor with identical membrane resistance and capacitance, as is the case for delayed rectifier conductances in blowflies (Heras et al., 2017). Activation of the Shaker conductance at low depolarizations and the Shab conductance at high depolarizations produces shunt peaking, which is again produced by delayed rectifier conductances in blowflies (Heras et al., 2016). Shunt peaking is produced by voltage-dependent ion channels changing their conductance with membrane potential after a delay, causing them to act like an inductance. This increases bandwidth without decreasing membrane gain, thereby increasing the photoreceptor membrane gain-bandwidth product (GBWP). The combination of the decrease in gain by negative feedback and the increase in GBWP by shunt-peaking caused by voltage-dependent K^+ conductances produces an increase in bandwidth without incurring the full cost that reducing the membrane resistance of a passive membrane would produce. Consequently, voltage-dependent conductances modify the trade-offs between membrane bandwidth, gain and energy cost by making it cheaper to operate a membrane with lower gain and higher bandwidth.

4.2 Shaker and Shab inactivation generates positive feedback amplifying low frequencies and saving energy

Inactivation of both the Shaker and Shab conductances produces positive feedback that amplifies frequencies below 1 Hz and 2 Hz, respectively. Amplification at low light levels has previously been attributed to a 'window current' (Niven et al., 2003b; Juusola et al., 2003; Kauranen and Weckström, 2004). Window currents occur in some fruit fly photoreceptors (Frolov, pers. comm.), but our modelling shows that amplification is produced by inactivation of the Shaker conductance alone. This amplification occurs against a background of negative feedback from other conductances as well as activation of the Shaker conductance itself, and so does not exceed the membrane resistance in most photoreceptors. Amplification by the Shab conductance at high light levels has not, to our knowledge, been described before. This is small because Shab inactivation occurs at high light levels when input resistance is low, reducing the relative effect of feedback. Moreover, the Shab steady-state inactivation curve has a relatively shallow slope and is centred at $-25.7\,\mathrm{mV}$, outside the range of typical steady-state depolarisations.

The functional significance of low frequency amplification remains unclear. Indeed, low frequency attenuation by the light current (Juusola and Hardie, 2001) makes it likely that the amplification produced by the Shaker and Shab conductances has little or no impact upon signalling in fruit fly photoreceptors, and is merely a side effect of inactivation. Thus, the role of Shaker in fruit fly photoreceptors is similar to that in the dendrites of vertebrate interneurons; decreasing the amplitude and time-to-peak of depolarising postsynaptic potentials rather than amplifying them (Hoffman et al., 1997). Instead, our modelling suggests that by increasing bandwidth at low light levels whilst ensuring that high bandwidths do not occur at high light levels, Shaker conductance inactivation reduces energy consumption in comparison to an equivalent non-inactivating conductance (Figure 7), as Niven et al. (2003a) hypothesised. Indeed, inactivation of A-type conductances in dendrites (Hoffman et al., 1997) may also be linked to reducing energy consumption.

4.3 Feedback from molecular exchangers and pumps

Other molecular components of the photoreceptors such as the Na^+/Ca^{2+} exchanger, which has a time constant of 350 ms (Chu et al., 2013) that can produce positive feedback amplifying frequencies below 1 Hz. However, the fraction of Ca^{2+} in the light-induced current is only about 26% (Chu et al., 2013), so the contribution of this positive feedback would be small. This positive feedback is unlikely to affect bandwidth and gain because the light response filters low frequencies (Juusola and Hardie, 2001). For our modelling, we considered the Na^+/Ca^{2+} exchanger as a constant current at each steady-state depolarisation, while studying the response to small signals. Our models also incorporated the Na^+/K^+ pump as a constant current at each steady-state depolarisation, rather than incorporating the actual dynamics. This approximation is accurate for the Na^+/K^+ pump current because it's slow dynamics (seconds, see e.g. Jansonius, 1990) restricts its negative feedback to extremely low frequencies.

4.4 Modulation of voltage-dependent K^+ conductances adjusts investment in photoreceptor gain and bandwidth

Neuromodulators alter specific properties of the voltage-dependent K^+ conductances, shifting the trade-off between contrast gain and bandwidth in fruit fly photoreceptors. Light-dependent modulation (LDM) of the Shab conductance by PIP2 depletion, which shifts Shab activation to lower potentials (Krause et al., 2008), moves the

trade-off to favour higher bandwidths and lower peak voltage contrast gains. Conversely, the positive shift the voltage operating range of both the Shaker and Shab conductances caused by serotonin (Hevers and Hardie, 1995), moves the trade-off to favour lower bandwidths and higher peak voltage contrast gains. Likewise, Ca^{2+}/Calmodulin antagonists that decrease the Shab conductance (Peretz et al., 1998) also favours lower bandwidths and higher peak voltage contrast gains. Conversely, an increase in the Shab conductance would favour higher bandwidths and lower peak voltage contrast gains. So, modulators enable fruit fly photoreceptors to explore a greater region of the trade-off between peak voltage contrast gain and bandwidth. This enables photoreceptors to adjust gain or bandwidth depending on the prevailing conditions. Both shifts produced by products of the photocascade, PIP2 depletion and an increase in Shab conductance produced by an increase in Ca^{2+} (Krause et al., 2008; Peretz et al., 1998), sacrifice gain for bandwidth thereby contributing to light adaptation (Figure 14a). Serotonin (Hevers and Hardie, 1995) has the opposite effect, increasing gain at the cost of bandwidth potentially adjusting photoreceptors to low light levels.

By adjusting voltage-dependent conductances, these neuromodulatory changes also have implications for photoreceptor energy consumption. If the light-induced conductance is kept constant, the neuromodulatory effects of phototransduction cascade products (Krause et al., 2008; Peretz et al., 1998) that increase bandwidth also increase in energy consumption. Thus, they reinforce the ability of the membrane to produce high bandwidth only when it is needed. This allows photoreceptors to save energy by avoiding investing in high bandwidth when it is not needed. Conversely, serotonin (Hevers and Hardie, 1995) reduces bandwidth and decreases the energy consumption if the light-induced current is kept constant. For a given energy consumption, light-dependent modulation (LDM) by PIP2 depletion decreases the cost of bandwidth but increases the cost of gain (Figure 13b,c). Conversely, serotonin decreases photoreceptor bandwidth but increases gain (Figure 13b,c). Likewise, Ca^{2+}/Calmodulin antagonists also increase the energy cost of bandwidth and decreases the energy cost of gain. An increase in Ca^{2+}/Calmodulin also decreases the cost of bandwidth but increases the cost of gain. The presence of multiple voltage-dependent conductances combined with multiple neuromodulators allows the costs of gain and bandwidth to be adjusted in independent ways.

By shifting the balance between gain and bandwidth (Figure 14a) neuromodulators can change the contrast-gain-bandwidth product (cGBWP). However, they have little effect on the cost of the cGBWP (Figure 14b). This can be understood by considering that the cGBWP is the product of the membrane GBWP times the light current, while the energy cost is proportional to the depolarising current —which is dominated by the light current at all but the lowest light levels. Thus, the cost of cGBWP is proportional to the membrane GBWP. As GBWP tends to be restricted between 1.2 and 1.5 for most choices of conductances, the cost of cGBWP varies little upon depolarisation or conductance shifts.

4.5 Implications of the simplified model of the light-induced current

We used a simplified model of phototransduction in which the photocurrent follows photon absorption. This model fails to capture low frequency filtering by light adaptation and high frequency filtering by the finite width and latency dispersion of the photon bump (Wong et al., 1980; Wong et al., 1982). Indeed, in *Drosophila* photoreceptors the phototransduction cascade current has a bandwidth between two and five times lower than the membrane bandwidth (Juusola and Hardie, 2001).

Incorporating the light-induced current into the model allowed us to study photoreceptor gain in a more relevant way than with membrane impedance alone. If membrane impedance is decreased using negative feedback, no increase the light-induced current is needed to keep the membrane voltage steady. The decreased impedance reduces the membrane gain but, because the light-induced current is unchanged, the net result is a decrease in voltage contrast gain. Conversely, if the membrane impedance were decreased by reducing the membrane resistance, an increase in the light-induced current would be necessary to keep the membrane voltage steady. The net result would be that voltage contrast gain is unchanged. This illustrates the importance of the interplay between the light-induced current and the membrane impedance.

4.6 Implications for arthropod photoreceptors

Within the arthropods, neuromodulation of photoreceptors is widespread. Some of these neuromodulators target the voltage-dependent conductances, whereas others act on molecular components of photoreceptor phototransduction cascade. In the fruit fly (*Drosophila melanogaster*), both octopamine and dopamine can increase the latency of quantum bumps without changing the membrane properties (Chyb et al., 1999). Likewise, in the desert locust (*Schistocerca gregaria*) serotonin shifts photoreceptors from the day state in which they express a voltage-dependent K^+ conductance with delayed rectifier-like properties to the night state in which they express a rapidly inactivating voltage-dependent K^+ conductance (Cuttle et al., 1995), whereas nitric oxide and cGMP modify their light response (Schmachtenberg and Bicker, 1999). This combination of neuromodulators that adjust elements of the phototransduction cascade and the photoinsensitive membrane separately provides considerable flexibily within photoreceptors to match prevailing environmental conditions, ensuring that energy is invested in high bandwidths only when it is needed. Avoiding expenditure on high bandwidth when it is unnecessary is an important strategy for reducing the cost of vision. Such changes may be predicted rather than being generated by prevailing environmental conditions, such as in the horseshoe crab (*Limulus*) in which photoreceptors undergo 24-hour cyclic changes

in sensitivity caused by octopamine (for a review see Battelle, 1991).

4.7 Implications for neuromodulation

The effects of neuromodulators upon the dynamics of single neurons and neural circuits are well documented in both invertebrates and vertebrates (Harris-Warrick and Marder, 1991; Katz, 1999; Grillner, 2003). Whilst neuromodulatory effects on the performance of single neurons and neural circuits have been described extensively, to our knowledge, their impact upon the energy consumption has not. Our results show that the changes wrought by neuromodulators to voltage-dependent conductances, are likely to affect the energy consumption of neurons and neural circuits. Indeed, many changes caused by neuromodulators, such as to sensory or synaptic inputs/outputs, or the reconfiguration of neural circuits, have implications for neuronal energy consumption. Although some changes may increase or decrease overall energy consumption, our findings suggest that the impact may be more subtle; neuromodulators may redistribute energy investment in different aspects of neuronal performance without substantially altering overall energy consumption.

Mechanoreceptors demonstrate the potential for neuromodulators to adjust or redistribute neuronal energy consumption. Neuromodulators can adjust numerous properties of invertebrate mechanoreceptors including their firing rate, dynamics, sensitivity and spike timing precision (Pasztor and Bush, 1987; El Manira et al., 1991; Zhang et al., 1992; Ramirez et al., 1993; Rossi-Durand, 1993; Matheson, 1997; Birmingham et al., 2003; Widmer et al., 2005; Billimoria et al., 2006). Although in many cases the underlying causes of these changes are unknown, in some they are linked to changes in conductance. For example, in the crab (*Carcinus maenas*) neuromodulation by allatostatin or serotonin of mechanoreceptors can adjust their spike rates and spike timing precision through changes in conductance; high conductance states are associated with lower spike rates and higher spike timing precision (Billimoria et al., 2006). In such cases, there will be implications both for the energy consumption of the neuron and for the cost of information coding. High conductance states to increase spike timing precision caused by allatostatin will likely increase the energy consumption of spikes and of maintaining the resting potential but the accompanying reduction in spike rate may reduce energy consumption (Billimoria et al., 2006). In these mechanoreceptors, serotonin has the opposite effect producing a low conductance, high spike rate state. Thus, as in fruit fly photoreceptors, neuromodulators in crab mechanoreceptors may redistribute the energy invested in different aspects of neuronal coding.

The ability of neuromodulators to redistribute the energy invested in different aspects of neuronal performance, and potentially to adjust the overall energy expenditure, has implications not only for single neurons but also for neural circuits. There are potential energy savings to the reconfiguration of neural circuits by neuromodulators to generate different behavioural outputs. The reuse of neurons to generate different behaviours reduces the need to build and maintain additional neurons, which would reduce energy consumption (Niven and Chittka, 2010). Neuromodulators may also redistribute energy investment in different parts of neural circuits. Indeed, neuromodulation may allow concerted changes in neurons and across neural circuits to co-ordinate investment in different aspects of neural processing to match prevailing behavioural and environmental circumstances.

5 Acknowledgments

The authors thank SB Laughlin, M Lengyel and DG Stavenga for discussion and feedback on previous versions of the manuscript.

FJHH was supported by Fundación Caja Madrid, The Department of Zoology of the University of Cambridge and Trinity College. JEN was supported by the BBSRC (grant number BB/R005036/1).

References

Abou Tayoun, A. N., X. Li, B. Chu, R. C. Hardie, M. Juusola, and P. J. Dolph (2011). "The Drosophila SK Channel (dSK) Contributes to Photoreceptor Performance by Mediating Sensitivity Control at the First Visual Network". In: *J Neurosci* 31.39, pp. 13897–13910.

Battelle, B.-A. (1991). "Regulation of retinal functions by octopaminergic efferent neurons in Limulus". In: *Prog Ret Res* 10, pp. 333–355.

Billimoria, C. P., R. A. DiCaprio, J. T. Birmingham, L. F. Abbott, and E. Marder (2006). "Neuromodulation of spike-timing precision in sensory neurons." In: *J Neurosci* 26.22, pp. 5910–5919.

Birmingham, J. T., C. P. Billimoria, T. R. DeKlotz, R. A. Stewart, and E. Marder (2003). "Differential and history-dependent modulation of a stretch receptor in the stomatogastric system of the crab, Cancer borealis". In: *J Neurophysiol* 90.6, pp. 3608–3616.

Chu, B., M. Postma, and R. C. Hardie (2013). "Fractional Ca2+ Currents through TRP and TRPL Channels in Drosophila Photoreceptors". In: *Biophys J* 104.9, pp. 1905–1916.

Chyb, S., W. Hevers, M. Forte, W. J. Wolfgang, Z. Selinger, and R. C. Hardie (1999). "Modulation of the Light Response by cAMP inDrosophila Photoreceptors". In: *J Neurosci* 19.20, pp. 8799–8807.

Cuttle, M. F., W. Hevers, S. B. Laughlin, and R. C. Hardie (1995). "Diurnal modulation of photoreceptor potassium conductance in the locust". In: *J Comp Physiol A* 176.3, pp. 307–316.

El Manira, A, C Rossi-Durand, and F Clarac (1991). "Serotonin and proctolin modulate the response of a stretch receptor in crayfish". In: *Brain Res* 541.1, pp. 157–162.

Gerster, U., D. G. Stavenga, and W. Backhaus (1997). "Na+/ K+-pump activity in photoreceptors of the blowfly Calliphora : a model analysis based on membrane potential measurements". In: *J Comp Physiol A* 180.2, pp. 113–122.

Gerster, U. (1997). "A quantitative estimate of flash-induced Ca2+- and Na+-influx and Na+/Ca2+-exchange in blowfly calliphora photoreceptors". In: *Vis Res* 37.18, pp. 2477–2485.

Grillner, S. (2003). "The motor infrastructure: from ion channels to neuronal networks". In: *Nat Rev Neurosci* 4.7, pp. 573–586.

Hardie, R. C. (1991). "Voltage-sensitive potassium channels in Drosophila photoreceptors". In: *J Neurosci* 11.10, pp. 3079–3095.

Harris-Warrick, R. M. and E. Marder (1991). "Modulation of Neural Networks for Behavior". In: *Annu Rev Neurosci* 14.1, pp. 39–57.

Heras, F. J. H., S. B. Laughlin, and J. E. Niven (2016). "Shunt peaking in neural membranes". In: *J R Soc Interface* 13.124, p. 20160719.

Heras, F. J. H., J. Anderson, S. B. Laughlin, and J. E. Niven (2017). "Voltage-dependent K+ channels improve the energy efficiency of signalling in blowfly photoreceptors". In: *J R Soc Interface* 14.129.

Hevers, W. and R. C. Hardie (1995). "Serotonin modulates the voltage dependence of delayed rectifier and Shaker potassium channels in drosophila photoreceptors". In: *Neuron* 14.4, pp. 845–856.

Hodgkin, A. L. and A. F. Huxley (1952). "A quantitative description of membrane current and its application to conduction and excitation in nerve". In: *J Physiol* 117.4, pp. 500–544.

Hoffman, D. A., J. C. Magee, C. M. Colbert, and D. Johnston (1997). "K+ channel regulation of signal propagation in dendrites of hippocampal pyramidal neurons". In: *Nature* 387.6636, p. 869.

Hryshko, L. V., S. Matsuoka, D. A. Nicoll, J. N. Weiss, E. M. Schwarz, S. Benzer, and K. D. Philipson (1996). "Anomalous regulation of the Drosophila Na(+)-Ca2+ exchanger by Ca2+." In: *J Gen Physiol* 108.1, pp. 67–74.

Immke, D., M. Wood, L. Kiss, and S. J. Korn (1999). "Potassium-dependent Changes in the Conformation of the Kv2.1 Potassium Channel Pore". In: *J Gen Physiol* 113.6, pp. 819–836.

Jansonius, N. M. (1990). "Properties of the sodium pump in the blowfly photoreceptor cell". In: *J Comp Physiol A* 167.4, pp. 461–467.

Juusola, M. and R. C. Hardie (2001). "Light Adaptation in Drosophila Photoreceptors I. Response Dynamics and Signaling Efficiency at 25C". In: *J Gen Physiol* 117.1, pp. 3–25.

Juusola, M., J. E. Niven, and A. S. French (2003). "Shaker K+ Channels Contribute Early Nonlinear Amplification to the Light Response in Drosophila Photoreceptors". In: *J Neurophysiol* 90.3, pp. 2014–2021.

Katz, P. S. (1999). *Beyond neurotransmission : neuromodulation and its importance for information processing.* Oxford University Press.

Kauranen, M. and M. Weckström (2004). "K+ Channels and Their Modulation by 5-HT in Drosophila Photoreceptors: A Modelling Study". In: *Ann Biomed Eng* 32.11, pp. 1580–1595.

Kety, S. S. (1957). "The general metabolism of the brain in vivo". In: *Metabolism of the Nervous System.* Ed. by D. Richter. Pergamon, pp. 221–237.

Koch, C. (1984). "Cable theory in neurons with active, linearized membranes". In: *Biol Cybern* 50.1, pp. 15–33.

— (2004). *Biophysics of Computation: Information Processing in Single Neurons.* Oxford University Press, USA.

Krause, Y., S. Krause, J. Huang, C.-H. Liu, R. C. Hardie, and M. Weckström (2008). "Light-Dependent Modulation of Shab Channels via Phosphoinositide Depletion in Drosophila Photoreceptors". In: *Neuron* 59.4, pp. 596–607.

Laughlin, S. B. (2001). "Energy as a constraint on the coding and processing of sensory information". In: *Curr Opin Neurobiol* 11.4, pp. 475–480.

Laughlin, S. B., R. R. de Ruyter van Steveninck, and J. C. Anderson (1998). "The metabolic cost of neural information". In: *Nat Neurosci* 1.1, pp. 36–41.

Marder, E. (2011). "Variability, compensation, and modulation in neurons and circuits." In: *PNAS* 108 Suppl 3.Supplement 3, pp. 15542–8.

Marder, E., T. O'Leary, and S. Shruti (2014). "Neuromodulation of Circuits with Variable Parameters: Single Neurons and Small Circuits Reveal Principles of State-Dependent and Robust Neuromodulation". In: *Annu Rev Neurosci* 37.1, pp. 329–346.

Matheson, T. (1997). "Octopamine modulates the responses and presynaptic inhibition of proprioceptive sensory neurones in the locust Schistocerca gregaria". In: *J Exp Biol* 200.9, pp. 1317–1325.

Minke, B. and E. Armon (1984). "Activation of electrogenic Na-Ca exchange by light in fly photoreceptors". In: *Vis Res* 24.2, pp. 109–115.

Niven, J. E., M. Vähäsöyrinki, and M. Juusola (2003a). "Shaker K+-channels are predicted to reduce the metabolic cost of neural information in Drosophila photoreceptors". In: *Proc R Soc Lond B* 270.Suppl 1, S58–S61.

Niven, J. E. (2016). "Neuronal energy consumption: biophysics, efficiency and evolution". In: *Curr Opin Neurobiol* 41. Microcircuit computation and evolution, pp. 129 –135.

Niven, J. E. and L. Chittka (2010). "Reuse of identified neurons in multiple neural circuits". In: *Behav Brain Sci* 33.4, pp. 285–285.

Niven, J. E. and S. B. Laughlin (2008). "Energy limitation as a selective pressure on the evolution of sensory systems". In: *J Exp Biol* 211.11, pp. 1792–1804.

Niven, J. E., M. Vähäsöyrinki, M. Kauranen, R. C. Hardie, M. Juusola, and M. Weckström (2003b). "The contribution of Shaker K+ channels to the information capacity of Drosophila photoreceptors". In: *Nature* 421.6923, pp. 630–634.

Niven, J. E., J. C. Anderson, and S. B. Laughlin (2007). "Fly Photoreceptors Demonstrate Energy-Information Trade-Offs in Neural Coding". In: *PLoS Biol* 5.4, e116.

Nusbaum, M. P. and M. P. Beenhakker (2002). "A small-systems approach to motor pattern generation". In: *Nature* 417.6886, pp. 343–350.

Pasztor, V. M. and B. M. Bush (1987). "Peripheral modulation of mechanosensitivity in primary afferent neurons". In: *Nature* 326.6115, p. 793.

Peretz, A., I. Abitbol, A. Sobko, C.-F. Wu, and B. Attali (1998). "A Ca2+/Calmodulin-Dependent Protein Kinase Modulates Drosophila Photoreceptor K+ Currents: A Role in Shaping the Photoreceptor Potential". In: *J Neurosci* 18.22, pp. 9153–9162.

Ramirez, J.-M., A Büschges, and R Kittmann (1993). "Octopaminergic modulation of the femoral chordotonal organ in the stick insect". In: *J Comp Physiol A* 173.2, pp. 209–219.

Rossi-Durand, C. (1993). "Peripheral proprioceptive modulation in crayfish walking leg by serotonin". In: *Brain Res* 632.1-2, pp. 1–15.

Schmachtenberg, O. and G. Bicker (1999). "Nitric oxide and cyclic GMP modulate photoreceptor cell responses in the visual system of the locust". In: *J Exp Biol* 202.1, pp. 13–20.

Skou, J. C. (1957). "The influence of some cations on an adenosine triphosphatase from peripheral nerves". In: *Biochimica et Biophysica Acta* 23, pp. 394–401.

Vähäsöyrinki, M., J. E. Niven, R. C. Hardie, M. Weckström, and M. Juusola (2006). "Robustness of Neural Coding in Drosophila Photoreceptors in the Absence of Slow Delayed Rectifier K+ Channels". In: *J Neurosci* 26.10, pp. 2652–2660.

Wang, T., H. Xu, J. Oberwinkler, Y. Gu, R. C. Hardie, and C. Montell (2005). "Light Activation, Adaptation, and Cell Survival Functions of the Na+/Ca2+ Exchanger CalX". In: *Neuron* 45.3, pp. 367–378.

Weckström, M. and S. B. Laughlin (1995). "Visual ecology and voltage-gated ion channels in insect photoreceptors". In: *Trends Neurosci* 18.1, pp. 17–21.

Weimann, J. M. and E. Marder (1994). "Switching neurons are integral members of multiple oscillatory networks". In: *Curr Biol* 4.10, pp. 896–902.

Widmer, A., U. Höger, S. Meisner, A. S. French, and P. H. Torkkeli (2005). "Spider peripheral mechanosensory neurons are directly innervated and modulated by octopaminergic efferents". In: *J Neurosci* 25.6, pp. 1588–1598.

Wong, F., B. W. Knight, and F. A. Dodge (1980). "Dispersion of latencies in photoreceptors of Limulus and the adapting-bump model." In: *J Gen Physiol* 76.5, pp. 517–537.

— (1982). "Adapting bump model for ventral photoreceptors of Limulus." In: *J Gen Physiol* 79.6, pp. 1089–1113.

Zhang, B., P. Torkkeli, and A. French (1992). "Octopamine selectively modifies the slow component of sensory adaptation in an insect mechanoreceptor". In: *Brain Res* 591.2, pp. 351–355.